Distribution Agreement

In presenting this thesis as a partial fulfillment of the requirements for a degree from Emory University, I hereby grant to Emory University and its agents the non-exclusive license to archive, make accessible, and display my thesis in whole or in part in all forms of media, now or hereafter now, including display on the World Wide Web. I understand that I may select some access restrictions as part of the online submission of this thesis. I retain all ownership rights to the copyright of the thesis. I also retain the right to use in future works (such as articles or books) all or part of this thesis.

Ruoyu Li April 5, 2024

Fluorescence Spectroscopy to Investigate the Effect of End-tethered Chains and Loops on the Local Glass Transition Temperature of Polystyrene Thin Films

by

Ruoyu Li

Connie B. Roth
Advisor

Physics

Connie B. Roth
Advisor

Jed Brody
Committee Member

Jennifer Rieser
Committee Member

2024

Fluorescence Spectroscopy to Investigate the Effect of End-tethered Chains and Loops on the Local Glass Transition Temperature of Polystyrene Thin Films

By

Ruoyu Li

Connie B. Roth

Advisor

An abstract of
a thesis submitted to the Faculty of Emory College of Arts and Sciences
of Emory University in partial fulfillment
of the requirements of the degree of
Bachelor of Science with Honors

Physics

2024

Abstract

Fluorescence Spectroscopy to Investigate the Effect of End-tethered Chains and Loops on the Local Glass Transition Temperature of Polystyrene Thin Films

By Ruoyu Li

I investigated the effect of grafted monocarboxy-terminated polystyrene (PS-COOH) chains and dicarboxy-terminated polystyrene (HOOC-PS-COOH) loops grafted to silica substrates on the local glass transition temperature (T_g) of 12 nm thick PS layers intermixed with the grafted polymers, and capped by a 590 nm bulk PS layer. T_g was measured via fluorescence spectroscopy, using pyrene dye copolymerized to PS as the probe. Temperature of the sample was ramped down steadily at 1 ^{o}C/min. T_g was located by identifying the change in slope of the linear dependence of fluorescence intensity vs. temperature. Overall, I found that the local T_g next to 50 and 100 kg/mol end-grafted chains increases by approximately 41 ± 2^oC independent of the grafting density compared to the T_g next to bare silica substrates, which is equal to $T_{g,bulk}$. These results contributed to a publication with James Merrill, a graduate student of our lab [J.H. Merrill, R. Li and C.B. Roth, *ACS Marco Lett.*, **2023**, 12, 1-7]. As for the loops, I found that the local T_g next to 50 and 100 kg/mol grafted loops increase by 36 ± 2^oC and 27 ± 2^oC compared to $T_{g,bulk}$, respectively, independent of the intermixing time between the 12 nm thick pyrene-labeled PS layer and the grafted loops. In addition, together with a current graduate student in our lab, James Merrill, we found a broad transition when analyzing the intensity vs. temperature data collected over a wide temperature range, which was characterized by identifying a lower T_g, denoted as T_g^{mid}. T_g^{mid} is still elevated compared to $T_{g,bulk}$, and is around 115^oC next to 50 and 100 kg/mol grafted loops, and varies between 113^oC and 130^oC for 50 and 100 kg/mol grafted chains. The difference $\Delta T_g = T_g - T_g^{mid}$ may inform about the breadth of glass transition, but its physical significance is yet to be determined.

Fluorescence Spectroscopy to Investigate the Effect of End-tethered Chains and Loops on the Local Glass Transition Temperature of Polystyrene Thin Films

By

Ruoyu Li

Connie B. Roth

Advisor

A thesis submitted to the Faculty of Emory College of Arts and Sciences
of Emory University in partial fulfillment
of the requirements of the degree of
Bachelor of Sciences with Honors

Physics

2024

Acknowledgements

I joined Professor Roth's lab in the spring semester of my freshmen year, and have had very meaningful times working in the lab. From my first email to request to join her lab three years ago, to the word-by-word level revision of this thesis today, Professor Roth has guided me with great meticulousness and offered me ample opportunity to refine my research skills. Her dedication to fostering a stimulating academic environment and commitment to my academic and personal growth have been instrumental in my development as an independent researcher.

I am particularly grateful to Jamie Merrill, who taught me all the experimental techniques I need to master when I first entered the lab, and patiently answered my questions in detail. When I encountered a problem in the course of my research, Jamie would generously offer assistance. Many of my experiments would not generate good data without his troubleshooting. I also want to thank the other members of the lab: Sunmin Kim, Sarita Yadav, Will Presson and Alex Couturier for their camaraderie. My time working in the lab would have been much less enjoyable without our funny conversations and mutual support.

Furthermore, I want to thank Professor Jed Brody and Jennifer Rieser for serving as members of my thesis committee, and for teaching me advanced laboratory and computational modeling classes. You helped me sharpen my physics skills and prepared me well for my future studies.

Table of Contents

List of Figures

CHAPTER 1
INTRODUCTION AND BACKGROUND

1.1 Introduction of Polymers and the Polymer Glass Transition

Polymers are carbon-based organic molecules with numerous repeat units, manufactured by combining single units, called monomers, into a long molecular chain via polymerization.[1] Polymers have widespread use in many fields, such as adhesives, rubber tires and additives to other materials to achieve desirable properties.[1] Polymers typically form a glass on cooling. In essence, glasses are non-equilibrium materials that result from packing frustration, where the glass transition of polymers is related to the packing frustration of polymer segments.[2] Although polymers can undergo a thermodynamic transition at a temperature T_m, turning from a crystal state to a liquid state, or vice versa, this process is relatively easy to bypass.[2] Instead, polymers often undergo the glass transition at the glass transition temperature, T_g. Unlike the thermodynamic transition from the liquid to crystal state, the glass transition is a kinetic transition, where the polymer falls out of the equilibrium liquid state and enters the nonequilibrium glassy state. While there is little structural change at the molecular level when a polymer undergoes the glass transition, the mechanical properties of the polymer will change significantly. For instance, the modulus of a polymer increases by as much as 3 orders of magnitude upon transitioning from the rubbery melt to glassy state.[2] Figure 1.1(a) shows the modulus as a function of temperature for different molecular weights of polymers.

The thermal expansivity also decreases when the polymer changes from its equilibrium liquid to glassy state.[2] However, distinct from thermodynamic transitions such as melting, the glass transition of polymers can occur at more than one temperature. Figure 1.1(b) shows the specific volume of the polymer as temperature changes. When the polymer in its liquid state is cooled fast, the glass transition occurs at a temperature $T_{g,1}$, higher than when the polymer is cooled in

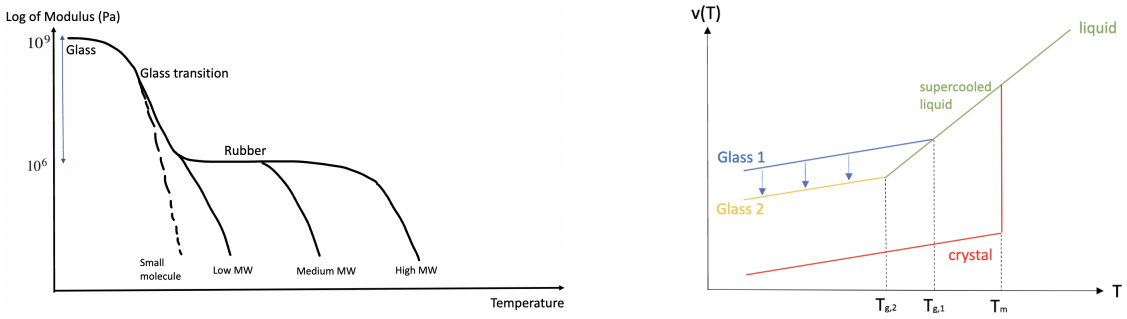

(a) (b)

Figure 1.1: Schematic diagrams representing (a) the temperature dependence of modulus for polymers of different molecular weights. Glass transition occurs when the modulus increases from 10^6 to 10^9 Pa, in which process the polymer changes from a polymer melt to a glass, and (b) the specific volume of the polymer as a function of temperature. Thermal expansivity, defined as $\frac{1}{V}(\frac{\partial V}{\partial T})_P$, is discontinuous at T_g. Moreover, $T_{g,1}$ corresponds to the glass formed at a faster rate of cooling, which will densify to glass 2 in the physical aging process.

the liquid state at a slower rate, when the system can maintain in equilibrium for longer and form a glass at a lower temperature $T_{g,2}$. After formation, glass undergoes physical aging, which is a gradual reduction of its volume as a function of time.[2] The thermal history of the system can be reset by heating the sample back to the equilibrium liquid state, and the physical aging of polymers is reversible.[2]

Microscopically, the polymer matrix can be visualized as many entangled chains. At very high temperatures, the chains behave like a simple liquid and form all possible configurations, known as the Arrhenius region. The activation energy for relaxation is hypothesized to be independent of temperature, and can be characterized by a simple Arrhenius temperature-dependence.[3]

$$\tau_\alpha \propto \exp(\frac{E_a}{k_B T}), \tag{1.1}$$

where k_B is the Boltzmann constant. Upon cooling in the liquid regime, if the polymer bypasses crystallization at temperature T_m, it enters a supercooled liquid state, where the system remains in equilibrium but cooperative motion sets in. Namely, the movement of individual polymer chains is hindered by the surrounding chains, and any flow or rearrangement requires the cooperative motion of multiple chains. The cooperatively rearranging region (CRR) is a small region of the

system undergoing collective motion, and is often treated as spherical for simplicity.[3] The size of the cooperatively rearranging region, $\xi_{CRR}(T)$, is roughly defined as the size of the collective molecular units that need to rearrange together at temperature T and is assumed to grow larger with decreasing temperature. Above T_g, glass formers such as polymers undergo α-relaxation, which is the structural rearrangement of polymer chain segments to return to equilibrium.[4] While the activation energy for α-relaxation is constant in the Arrhenius region, in the non-Arrhenius region, molecules have less available thermal energy, and larger CRRs require higher activation energy for α-relaxations. Hence, the time for α-relaxations can be modeled by

$$\tau_\alpha \propto \exp(\frac{E_a(T)}{k_B T}). \tag{1.2}$$

One interpretation of the temperature dependence of the timescale of the α-relaxation of the polymer chain matrix in the non-Arrhenius region is that the temperature-dependent activation energy $E_a(T)$ can be treated as $E_a(T) \propto zE_a^*$, where E_a^* is the activation energy of a single unit in the CRR, and z is the number of units that makes up the CRR.[2] By convention, T_g is the temperature when the time for α-relaxations reaches 100 seconds.[3] Therefore, in the glassy state, the polymer chains are essentially static, but macroscopically, the chains retain the amorphous structure as in the liquid state, with individual chains frozen in place. Figure 1.2 is a sketch of the time constant of α-relaxations against the inverse of temperature. Above the Arrhenius temperature T_A, the time constant of α-relaxations increase linearly with temperature, and when the temperature drops, the polymer enters the supercooled liquid state, the time for α-relaxations increase dramatically, implying large change in the dynamics of the molecules.[2]

In short, glass transition of polymers is kinetic as opposed to thermodynamic. Upon cooling from the liquid state to glassy state, the mechanical properties of the polymer change abruptly over a short temperature range, but there is little change in its structural properties. Glass transition can be affected by factors such as polymer film thickness, the interface between the polymer and the substrate, as well as the molecular weight of the polymers.[5] Polystyrene (PS) is widely used

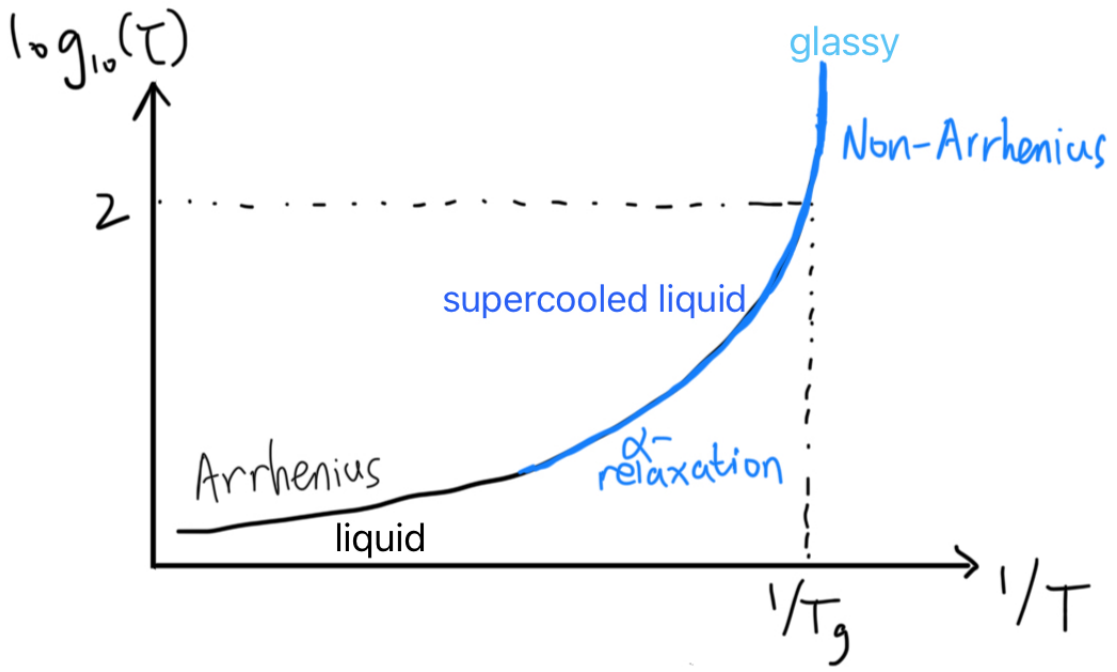

Figure 1.2: The time for α-relaxations as a function of 1/T. Time constant for α-relaxations reaches 100 seconds at the glass transition temperature.

for investigation of the polymer glass transition. The T_g of bulk PS increases with the degree of polymerization, and reaches the limiting value of around 100^oC for PS with molecular weight greater than 20 kg/mol,[2] and whose value will be denoted as $T_{g,bulk}$. However, for PS thin films, the interface plays a significant role in the glass transition temperature. When the thickness of the PS film is below 100 nm, the T_g decreases as a result of enhanced dynamics at the free surface, which extends several tens of nanometers into the film, and as the PS film thickness decreases, the T_g decreases correspondingly from $T_{g,bulk}$.[6]

1.2 The Effect of a Modified Interface on the Polystyrene Glass Transition Temperature

Apart from the thickness of the PS film, the interface between the substrate and the polymer can also lead to tunable interfacial properties. For example, small-molecule surfactants can reduce interfacial energy and elevate interfacial fracture toughness if carefully designed.[7] Polymer brushes, polymer chains with one end covalently-attached to the substrate, is a basic model to investigate various interfacial phenomena such as the glass transition.[8] Alternatively, polymer

chains can be physically deposited onto the substrate without covalent bonding, in a process called adsorption. The effect of adsorbed layers on the T_g of PS is more subtle and less well studied.[9]

1.2.1 Literature of How Grafted Chains Impact Polystyrene Glass Transition

A prototypical model of end-tethered (grafted) chains is the polymer 'brush', which are chains with one end covalently bonded to a planar substrate, and the other end free to move.[7] The conformation of end-grafted chains on the substrate is largely determined by the grafting density, which is the number of PS chains grafted onto the substrate per unit area, denoted σ. Assuming the grafted chains have the same bulk density without solvent, the grafting density is calculated as

$$\sigma = \frac{\rho N_A h_{brush}}{M_n}, \tag{1.3}$$

where ρ is the bulk density of the chains; N_A is the Avogadro's constant; h_{brush} is the thickness of the dry brush, and M_n is the number average molecular weight of the grafted polymers.[10] The reduced tethered density is a measure of surface coverage of the grafted chains on the substrate and is given by $\Sigma = \pi R_g^2 \sigma$, where R_g is the radius of gyration of the grafted chains.[10] The proposed conformation of polymer chains grafted onto the substrate is shown in Figure 1.3. For $\Sigma < 1$, the chains are isolated, meaning that the distance between the grafting points is greater than R_g. This is the "mushroom" regime, in which the grafted chains are isolated on the substrate analogous to a mushroom. As grafting density increases, the chains are no longer isolated and they can overlap with each other. This transition occurs approximately around $1 < \Sigma < 5$. In the limit of high grafting density, the chains become stretched out by steric hindrance and the system is in the "true brush" regime.[11]

When a PS thin film is placed above the grafted layer, the grafted chains interpenetrate with the PS matrix network.[12] The extent of intermixing depends on the difference in the molecular weight of the grafted and the matrix chains. Suppose the grafted chains have degree of polymerization N, when the molecular weight of the matrix chains is greater than $N^{\frac{1}{2}}$ and $\sigma < N^{\frac{1}{2}}$, the

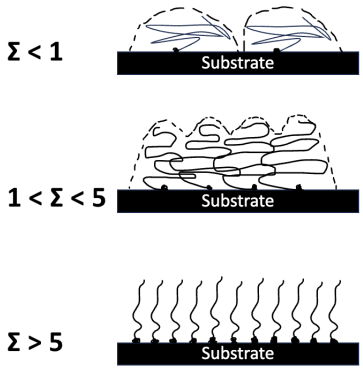

Figure 1.3: The proposed conformation of grafted chains under different grafting densities. In general, in the mushroom regime ($\Sigma < 1$), the chains are isolated and squashed onto the surface, and as the chains start to interact, they become stretched out as the grafting density increases. The reduced tethered density at which the chains stretch into brushes is an approximate value. In fact, the transition between different regimes is continuous and occurs over a range of Σ.

grafted chains will have a random walk chain conformation, with extent $L \approx aN^{\frac{1}{2}}$, where a is the size of a monomer.[13] While they interpenetrate the matrix chains, the end-grafted chains retain their ideal chain conformation from the mushroom regime all the way to the beginning of the true brush regime. As grafting density approaches unity, the grafted chains will fully stretch out and has thickness proportional to N, but the matrix chains will become expelled from the grafted layer, resulting in limited interpenetration because of the lack of free space.[13]

Ellison and Torkelson developed a method to measure the local T_g using the fluorescent label or dopant pyrene,[14] allowing the effect of grafted layers on T_g of PS to be determined easily. In a Nature Materials article, Ellison and Torkelson placed 12 nm or 14 nm thick pyrene-labeled PS layers at different locations: near the substrate while covered by a bulk layer, or near the free surface, and sandwiched top and bottom in between two bulk PS layers. Their measurement showed that the T_g of the pyrene-labeled PS layer close to the free surface with a bulk PS underlayer is 32 K lower than the layers without the free polymer-air interface, whose T_g is equal to $T_{g,bulk}$, and that the T_g of the PS layer reduces when the pyrene-labeled PS layer is within some tens of nanometers to the free surface.[6] Therefore, the interface plays a significant role in the T_g.

Due to the intermixing between grafted and matrix chains, the grafted layer may cause a difference in the dynamics of cooperative segmental motion of the matrix chains, hence resulting

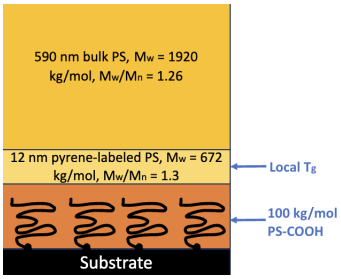

Figure 1.4: The multilayer sample geometry Xinru Huang used to study the impact of grafted layer on the local T_g of PS.[11] The grafted layer she used consistes of 100 kg/mol PS-COOH chains.

in different T_g of the matrix chains compared to the bulk value. There have been numerous studies on the effect of grafted layers on T_g. In 2017, Hénot et al. measured the average T_g across the thickness of the entire PS film by ellipsometry, and revealed insignificant change between the bare silicon substrate and grafted layers. They concluded that the T_g is likely not influenced by grafting, but by the free surface effect, so it appeared that the grafted layer has limited impact on the T_g of PS.[15] However, their measurement did not isolate the impact of the grafted layer. The free surface atop the PS film tend to lower the T_g, cancelling out the potential increase in T_g caused by the grafted layer. To isolate the effect of grafted layers, Xinru Huang, a previous graduate student in our lab, adopted a multilayer sample geometry that measures the local T_g of 12 nm thick pyrene-labeled PS placed atop the grafted substrate, and capped by a 590 nm thick bulk PS layer to eliminate free surface effect, as in Figure 1.4.[11] The local T_g of the 12 nm PS layer measured by fluorescence spectroscopy showed a maximum of 49 ± 2 K increase in T_g of a 12 ± 1 nm thick PS film atop substrate with grafted PS-COOH chains at an optimal grafting density in the mushroom-to-brush transition regime.[11]

1.2.2 Impact of How Adsorbed Layers Impact the Polystyrene Glass Transition

The effect of adsorbed layers on the local T_g can be studied by adopting the same multilayer sample geometry, but replacing grafted layers with adsorbed layers. Adsorbed layers are made by depositing polymer chains onto the substrate via immersion of the substrate in a toluene solution of the polymer, which is a relatively well-studied system,[9] or by annealing the polymer thin film

at elevated temperature under vacuum for some time, then rinsing with a pure solvent to wash away unadsorbed chains, called the Guiselin's experiment.[16] When adsorbed chains are bound to the substrate, the configuration of the polymer chains can be modeled as tails with a free end away from the substrate, trains in direct contact with the substrate interface, and loops that extend above the substrate then return. The loops extend halfway as far above the substrate as tails do, and then return to the substrate.[9] The thickness of solution-grown adsorbed layers depends on the concentration of the solution, and reaches a plateau value after a short immersion time in the solution.[7] Due to crowding of chains at the surface, a higher concentration of solution leads to shorter trains, longer tails and more fluffy loops, resulting in thicker layers; in contrast, lower concentrations of solution allow for more spreading of the chains on the surface, hence longer trains.[9]

The impact of adsorbed PS layers on the local T_g of PS thin films is more subtle than that of grafted layers, because different preparation protocols of the adsorbed layer lead to very different responses of measured T_g relative to the $T_{g,bulk}$. After intermixing the adsorbed layer with the pyrene-labeled PS layer for varying durations in 170^oC vacuum, it was demonstrated that solution-grown adsorbed layers do not lead to a significant elevation of the local T_g of the PS matrix, and even a reduction of the local T_g when both layers are intermixed for only 2 hours, probably due to the increased mobility of the matrix PS chains due to free volume trapped by large loops in the adsorbed layer.[9] However, for adsorbed layers formed by melt annealing at 150^oC for 23 hours and washing in pure toluene solvent for 30 minutes, it was found that 48-hour intermixing of the adsorbed layer and the probe layer contributes to a plateau value of $T_{g,bulk} + 30$ K of the local T_g of PS, while annealing time of 2 hours does not lead to significant rise in the local T_g.[9]

Multiple local T_g measurements with adsorbed layers prepared via different protocols were conducted to examine which of the adsorbed tails, trains or loops affect the T_g. For solution-grown adsorbed layers with $h_{ads} \approx 4.5$ nm, the local T_g remains within the error range of T_g of bulk PS even after 48 hours of intermixing with the matrix PS chains.[9] A likely interpretation of this finding is that the tails of adsorbed chains, unlike grafted chains, do not lead to elevated local

T_g of PS matrix chains. They also showed that after sufficiently long desorption, which is the immersion of the substrate with adsorbed chains in pure solvents for washing the chains off, the remnant chains on the substrate form a residual layer consisting of mostly trains, and that the local T_g above this residual layer is consistent with the $T_{g,bulk}$, indicating that the trains probably do not lead to elevation in T_g either.[9]

Therefore, a possible interpretation is that the observed elevation in the local T_g is caused by the intermixing of the matrix chains with the loops in the adsorbed layer. The timescale of this process depends on the rate of threading of the matrix PS chains through the loops, which is longer than the interpenetration of end-grafted chains, and hence an elevated T_g was observed after 24 hours and 48 hours of intermixing between the melt annealed adsorbed layer and the probe layer, but an intermixing time of two hours yielded a local T_g barely higher than $T_{g,bulk}$, indicating that two hours may be insufficient for threading to occur.[9]

The difference in the impact on the local T_g caused by solution-grown adsorbed layers and melt annealed layers is likely due to the size of the loop. adsorbed layers prepared by immersing the substrates in $c = 1.0$ mg/ml solution have $h_{ads} \approx 4.5$ nm, and are proposed to have fluffy loops and short trains. However, for melt-annealed adsorbed layers made with the same concentration of solution, a coarsening mechanism of trains is proposed based on the slow down in desorption rate for longer annealing time at 150^oC.[9] The authors hypothesize that melt annealing favors more polymer segment-surface contacts, and hence over prolonged annealing, the trains in the adsorbed PS chains will be longer, resulting in smaller and tighter loops.[9]

For solution grown layers, the little increase in the measured T_g after 48 hour intermixing indicates that T_g is independent of the degree of threading with fluffy loops. However, for melt annealed layers, which have tighter loops than solution grown layers, the measured T_g increases by as much as 30 K from $T_{g,bulk}$ after 48-hour intermixing, suggesting that threading of PS matrix chains with tight loops restricts the mobility of the matrix chains and hence elevates the local T_g, and that this process would take significantly longer than 2 hours.[9]

1.2.3 Summary of Previous Literature

In summary, previous literature has demonstrated that the grafted layer increases the local T_g of polystyrene films, suggesting the slowing down of the polymer segmental dynamics caused by the polystyrene end-grafted chains.[11] On the other hand, the presence of a free surface tends to lower the local T_g of the polystyrene thin film,[6] offsetting the effect of the grafted layer.[11] Therefore, the results suggest that, without a free surface, the grafted layer increases the local T_g of PS.

In the Thees et al. publication in the Journal of Chemical Physics, the authors drew a comparison between adsorbed layers and grafted layers, and deduced that adsorbed tight loops slow down the dynamics of PS chains after the PS chains thread through the loops, and that the trains, fluffy loops, and tails have limited effect on the T_g of PS.[9] Importantly, the timescale of intermixing between PS chains and tight loops can be long, so the local T_g depends strongly on the intermixing time.

1.3 Goals of the Project

In this study, following the previous research described in the literature, I characterized the effect of different grafted layers on the local T_g of 12 nm thick pyrene-labeled PS layers intermixed with the grafted chains. The grafted substrate consists of carboxy-terminated polystyrene (PS-COOH) chains covalently bonded to a substrate of optical quality quartz. Previous research of the impact of grafted layers on the T_g of PS done in our lab used $M_n = 98.8$ kg/mol PS-COOH chains for grafting onto the substrate, and measured the T_g dependence of grafting density on the T_g of PS. However, the grafting density dependence of local T_g of PS was minimally characterized. To reproduce the data published in their paper, I prepared substrates with varying grafting densities of 100 kg/mol PS-COOH chains and measured the local T_g. In addition, to eliminate the possibility of alternative causes of the rise in T_g. I did control measurements by measuring the local T_g of PS above bare quartz substrates, adopting slightly different preparation steps of the probe layer and

the assembly of the structure to see whether $T_{g,bulk}$ would be recovered.

The local T_g of PS may also depend on the molecular weight of the end-grafted chains. To investigate the impact of molecular weight of grafted chains on the local T_g of PS, in addition to the original 98.8 kg/mol PS-COOH, I used $M_n = 45.7$ kg/mol PS-COOH chains as the grafted layer, for which I also varied the grafting density and measured the local T_g of the pyrene-labeled PS layer. These results contributed to a paper that found that molecular weight of the grafted layer and the grafting density has limited effect on the local T_g of the PS layer.[17]

Inspired by the discoveries that adsorbed tight loops increase the local T_g after sufficiently long intermixing of the probe layer and the adsorbed layer, and that without intermixing, the T_g measured is roughly equal to $T_{g,bulk}$, I researched the impact of grafted loops on the local T_g of PS thin film to compare the impact of grafted and adsorbed chains on the local T_g of PS. In the second part of the project, which took place from August 2023 to March 2024, I progressed from grafting monocarboxy-terminated PS-COOH chains to grafting dicarboxy-terminated HOOC-PS-COOH onto the substrate, which forms ester bonds on both ends.

Loops have a different topological structure from end-grafted chains, and it was proposed that tight adsorbed loops lead to increases in the local T_g after sufficiently long intermixing between adsorbed and probe layers. The adsorbed layer is a complicated system. To study the impact of loops alone, I adopted the simple system of grafted loops, and to compare the effect of the size of loops on the local T_g, I grafted 50 kg/mol and 100 kg/mol loops and used the same multilayer sample geometry as in Xinru's paper. To estimate the timescale of threading of PS chains with the grafted loops, I chose the same intermixing durations as those chosen by Thees et al. to intermix the pyrene-labeled PS layer and the adsorbed layer.

Overall, these studies hopefully inform us about how different grafted layers alter the dynamics associated with the local cooperative segmental rearrangement of PS chains. These discoveries may provide some insight into the applications of grafted polymer chains and polymer nanocomposites (PNCs) to tailor the surface toughness and other properties of the interface, as well as improving the mechanical, thermal and optical properties of the material.[12,18,19]

CHAPTER 2
EXPERIMENTAL METHODS

2.1 Preparation of the Multilayer Sample

2.1.1 Preparation of Grafted Layers

The grafted layers were synthesized via the so-called 'grafting-to' technique, in which the preformed end-functionalized chains form covalent bonds with the complementary functional groups on the substrate.[10] The substrates were pieces of 25 mm by 25 mm optical quality quartz for fluorescence spectroscopy measurements and half-polished silicon wafers for measuring the thicknesses of the layers by ellipsometry. Since the silica substrates were reused multiple times, piranha cleaning was implemented after each measurement to remove any covalently bonded PS chains on the substrate. For safety reasons, this step was completed thanks to a graduate student in our lab, James Merrill. The piranha-cleaned substrates were then stored in deionized (DI) water until use. The samples were assembled layer by layer. The first part of this research aimed to investigate the impact of grafted monocarboxy-terminated polystyrene (PS-COOH), which forms one ester bond with the Si-OH groups on the substrate surface. Immediately prior to grafting, the quartz and silicon substrates were immersed into 1:2 mixture of 13 M hydrochloric acid (HCl) and DI water for 30 seconds, then rinsed in DI water, and blown dry with nitrogen (N_2) gas after each step.

Spin coating is a simple method of preparing thin films on a rotating substrate. An excess amount of polymer solution is added onto the substrate, which is held fixed onto a stage by vacuum. The substrate is then set spinning at a controlled angular velocity. In the course of spinning, the solvent evaporates, leaving a dry film on the substrate whose thickness is proportional to the inverse of the square root of spin speed.[20]

The grafted layer was prepared by spin-coating the solution of PS-COOH (M_n= 45.7

kg/mol, M_w/M_n=1.07 for 50 kg/mol grafted chains; M_n = 98.8 kg/mol, M_w/M_n = 1.03 for 100 kg/mol grafted chains)[17] in toluene directly onto the substrate. The time of spin coating was held at 45 seconds. Then, the grafted substrates were annealed at 170^oC under vacuum for 30 minutes to allow the formation of ester bonding. The thicknesses of the layer on the silicon substrates were measured on the ellipsometer. The substrates were then washed in 90^oC toluene for 20 minutes to remove ungrafted chains, and rinsed with acetone and deionized water, while dried with N_2 gas after each step. Finally, the samples were placed under vacuum at room temperature for overnight annealing. This results in the dry-brush thickness h_{brush} of the grafted layer, which was measured the following day on the ellipsometer.

For the second part of this research, which aimed to investigate the impact of grafted loops ($M_w \approx$ 50 kg/mol or 100 kg/mol, M_w/M_n not specified), the substrates were prepared in a similar manner, except that the polymer used was dicarboxy-terminated polystyrene (HOOC-PS-COOH), which could form two ester bonds with the substrate on both ends of the chain. However, a complication could arise when preparing grafted loops as it would be difficult to determine whether ester bonds form on both ends of the chain or only on one end. To focus on the impact of grafted loops, it would be optimal to have the substrate with all chains bonded on both ends, and not bonded on only one end, to the substrate. To address this, the annealing procedure for grafting loops onto the substrate was modified. The annealing time immediately after spin coating was lengthened to 2 hours to ensure that as many ester bonds form as possible. After the initial annealing, the film thickness was measured and the substrates were washed in toluene as with grafted chains. After washing away ungrafted chains, the substrates were annealed under 170^oC vacuum for an additional 30 minutes so that any remaining single-end grafted molecules would very likely form another bond with the substrate and become a loop. Then, the substrates were placed under vacuum at room temperature for overnight annealing, and the thickness of the grafted layer was measured, also denoted h_{brush}.

Slightly different from Equation 1.1, grafting density in the context of my project is calculated as $\sigma = \frac{n\rho N_A h_{brush}}{M_n}$, where n is the number of grafted points per chain: $n = 1$ for end-grafted

chains and $n = 2$ for grafted loops; ρ = 1.045 g/cm^3 for PS; N_A is the Avogadro's constant, and M_n is the number average molecular weight of the grafted polymer (98.8 kg/mol or 45.7 kg/mol). The grafting density depends on spin speed and the concentration of the grafted layer solution. Together, they determine the initial thickness of the spin-coated film of grafted chains.

2.1.2 Preparation of Pyrene-labeled PS Layer, the Bulk PS Layer and Their Assembly

The probe of the glass transition is a pyrene-labeled PS (M_w = 672 kg/mol, M_w/M_n=1.3), which is styrene copolymerized with 1-pyrenyl butylmethacrylate, with 1.4 mol % pyrene content.[11] This pyrene-labeled PS was dissolved in toluene with a concentration of 0.3% by weight, and then spin-coated onto half-cleaved mica to form approximately 12 nm thick fluorescent probe layers. First, a film would be spin-coated onto a silicon substrate, and then the thickness of the film would be measured by ellipsometry. After noting the thickness of the film produced at a particular spin speed, the desired spin speed for the desired thickness could be calculated given the relationship between spin speed and film thickness.

The layers were then annealed under vacuum at 120^oC overnight to remove the residual solvent, and then crosslinked with 254 nm UV light at a distance of 16 mm above the film for 10 minutes at room temperature in order to prevent the diffusion of the chains in the layer at high temperatures.[11] The probe layer was transferred from the mica substrate onto the silica substrate with the grafted layer using a water transfer process: Upon slowly dipping the mica substrate into a DI water bath, there is a capillary-induced peeling force at the edge of the hydrophobic thin film.[21] The film will ultimately separate from the mica substrate and float on the water surface, and can be deposited onto the silica substrate.

After transferring the probe layer, the bilayer structure was annealed at 170^oC under vacuum to ensure intermixing of the pyrene-labeled PS and the grafted chains covalently bonded to the substrate. For PS end-grafted chains, which intermix with the probe layer via chain extension and retraction breathing modes,[12] 2 hours of annealing is sufficient.[11] For grafted loops, whose topological structure is different from end-grafted chains, the interpenetration of the matrix chains

with the grafted layer depends on the threading of the matrix chains with the loops, the timescale of which process can be much longer. Based on the experimental method outlined in investigating the impact of film annealed adsorbed layers on T_g, an annealing time of 24-48 hours appears to be sufficient to reach a plateau in T_g value.[9] Following their annealing protocols to intermix adsorbed layers and the probe layer, the bilayer structures of grafted and probe layers were annealed for 2 hours, 24 hours and 48 hours at 170^oC vacuum for intermixing.

In order to isolate the effect of the grafted layer on the glass transition of the ultrathin PS film, we placed a 590 ± 5 nm bulk PS layer (M_w = 1920 kg/mol, M_w/M_n = 1.26) on top of the probe layer. Similar to the probe layer, the bulk PS layer was spin-coated onto mica substrates, and annealed under vacuum at 120^oC overnight, then floated atop the probe layer using the same water transfer process to float the probe layer before T_g measurement on the spectrofluorometer. This would result in the multilayer sample geometry as shown in Figure 2.1:

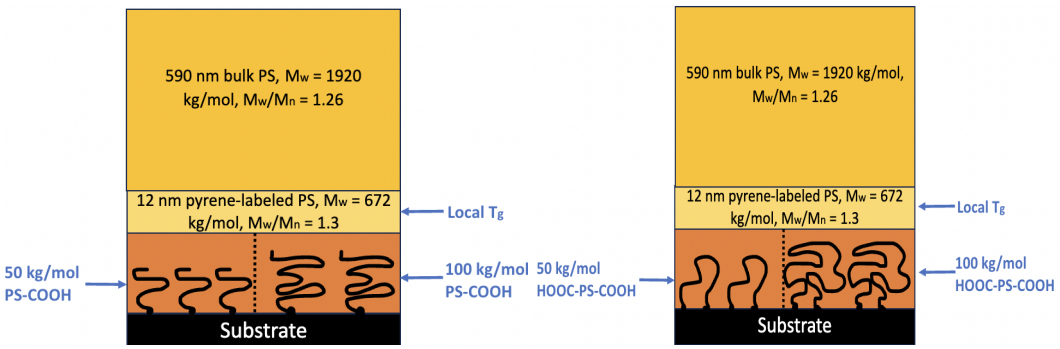

(a) (b)

Figure 2.1: The multilayer sample geometry used in my research are similar to the sample geometry Xinru used, but with different grafted layers. In (a), the grafted layer consists of 50 kg/mol or 100 kg/mol PS-COOH chains, and in (b) the grafted layer consists of 50 kg/mol or 100 kg/mol HOOC-PS-COOH loops. The effect of different grafted layers on the local T_g is compared.

2.1.3 Measuring the Thicknesses of the Layers via Ellipsometry

In preparing the probe layers and the bulk PS cap layer, prior to spin coating onto mica, one sample would be spin coated onto silicon substrates to measure the thickness of the layers by ellipsometry. The thickness measured at a given spin speed could serve as a reference. Given that

the thickness of films made via spin coating is found to be inversely proportional to the square root of spin speed,[20] the spin speed needed to produce films of the desired thickness could be calculated.

An ellipsometer (Woollam M-2000) was used to measure h_{brush} of the grafted layers and the thicknesses of the probe layers and the bulk PS caps. The film was treated as an optical layer model, consisting of a standard Cauchy layer for the polymer film with thickness h and wavelength-dependent refractive index $n(\lambda)$ can be described by $n(\lambda) = A + \frac{B}{\lambda^2} + \frac{C}{\lambda^4}$, where A, B, and C are the optical constants of the polymer film. Other than the polymer film, there is a native oxide layer above the silicon substrate of thickness 1.4 nm.[17] and the silicon wafer is treated as semi-infinitely thick. When light hits the interface between each of these layers, some is reflected and some is transmitted. Fresnel reflection coefficients relate the electric field component of the light in each medium, and the thickness of the polymer film, h and the index of refraction, n can be derived from the total Fresnel reflection coefficient.[22] The ellipsometer emits broad spectrum light where the wavelengths λ from 400 to 1000 nm are analyzed at an incidence angle with respect to the normal of the film. $\Psi(\lambda)$ and $\Delta(\lambda)$, which are the principal angles of ellipsometry, represent the changes in amplitude and phase difference of the orthogonal components of the electric field of the emitted and reflected light.[22] The electric field vector can be decomposed into $\vec{E_p}$ and $\vec{E_s}$ to denote the component parallel and perpendicular to the plane of incidence, respectively. The fundamental equation of ellipsometry is

$$\rho = \tan(\Psi)e^{i\Delta} = \frac{r_{tot}^p}{r_{tot}^s}, \tag{2.1}$$

where the coefficients r_{tot}^p and r_{tot}^s represent the p- and s-components of the total Fresnel reflection coefficient.[22]

The ellipsometer measures the intensity of the parallel and perpendicular components of the reflected light, I^p and I^s, which satisfies $\frac{I^p}{I^s} = \frac{|r_{tot}^p|^2}{|r_{tot}^s|^2} = |\rho|^2$. Upon measuring Ψ and Δ, the ellipsometer compares the ρ values predicted by the optical layer model with the experimentally obtained values, and generates the fits for the parameters A, B, and C, as well as the film thickness h, by minimizing the mean squared error (MSE) between the theoretical and the experimental values of $\Psi(\lambda)$ and $\Delta(\lambda)$.[23] For measuring the dry-brush thickness of a grafted layer, which is

typically less than 10 nm, $\Psi(\lambda)$ and $\Delta(\lambda)$ were collected at three angles of incidence, with 5 seconds at each of 55^o, 60^o and 65^o. For grafted layers, A, B, and C were kept fixed at the bulk value for PS, and only the film thickness h was fitted.[17] The thickness of each film was measured on three different spots, and the average value was taken as the thickness h.

2.2 Fluorescence Spectroscopy to Probe the Glass Transition Temperature

This section will focus on fluorescence theory and technique, how it is used to sense the glass transition, and the central role fluorescence has in our project. The fluorescence T_g technique usually involves a label, which is copolymerized with the polymer, or a dopant, which is mixed into the polymer matrix without covalent bonding. Information such as the glass transition temperature can be revealed by studying the fluorescence emission spectra.

Pyrene, an aromatic molecule consisting of four benzene rings, is a good fluorophore due to its long lifetime of 450 ns and decent quantum yield of 0.65.[24] The emission intensity of pyrene is highly dependent on the surrounding chemical environment. Upon changing from liquid state to glassy state, there is a break in the linear temperature dependence of fluorescence intensity of pyrene. Therefore, the T_g of a polymer thin film system can be determined by adding pyrene labels into the polymer system and then implementing fluorescence spectroscopy.[14] Figure 2.2 is a sketch of the structure of pyrene dye copolymerized with styrene monomers for sensing the T_g.

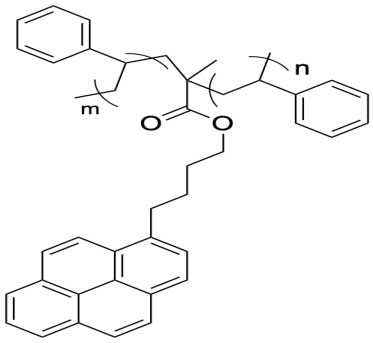

Figure 2.2: The chemical structure of the probe of glass transition, the pyrene-labeled PS, which is 1-pyrenylbutyl methacrylate copolymerized at trace levels with styene monomers.[17]

With four benzene rings, pyrene is rich in C=C double bonds, of which one is a σ bond, and

the other is a π bond. In the ground state, S_0, the p-orbitals of the two carbon atoms in the π bond are aligned, but upon excitation, pyrene undergoes $\pi - \pi^*$ electronic transition, and the p-orbitals of the two carbon atoms become anti-aligned, resulting in an unstable π^* bond. Figure 2.3 is a schematic diagram showing the change in bonding as the result of the transition and the associated change in energy level. The transition results in the pyrene molecule going to the second singlet excited state, S_2.[24] The excitation wavelength contributing to this transition is around 330 nm,[14] although previous researches have used excitation wavelengths of 322 nm or 340 nm[5,6].

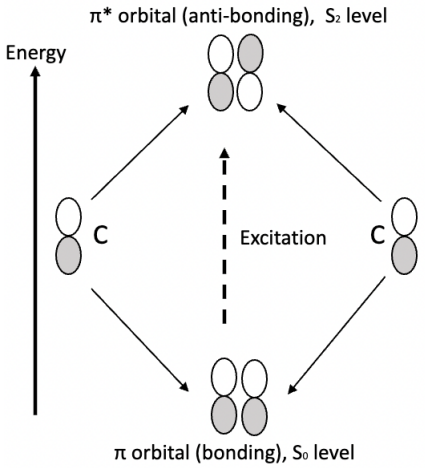

Figure 2.3: Schematic diagram showing the π to π^* transition of electrons in a C=C bond

Excited pyrene quickly returns to its ground state. Since there are fine splittings within a singlet state, the emitted photons have a spectrum of wavelengths, with two prominent peaks between 370 and 410 nm. The highest peak of emission intensity at high temperature is around 379 nm. Figure 2.4 are the emission spectra of pyrene, showing the emission intensities of pyrene emission at room temperature, 130^oC, and 170^oC, using a sample with pyrene-labeled PS layer placed on top of the substrate without grafted layer.

Fluorescence is the emission of light when a fluorophore in its singlet electronically excited states returns to the ground state. The emission rate of fluorescence is typically $10^8 \mathrm{s}^{-1}$.[25] Upon excitation with photons of a specific frequency, specific electrons in the molecule will move to a higher energy level. Within their excited energy levels, the electrons undergo internal conversion, which is the relaxation to the lowest vibrational and/or rotational state in that level, at

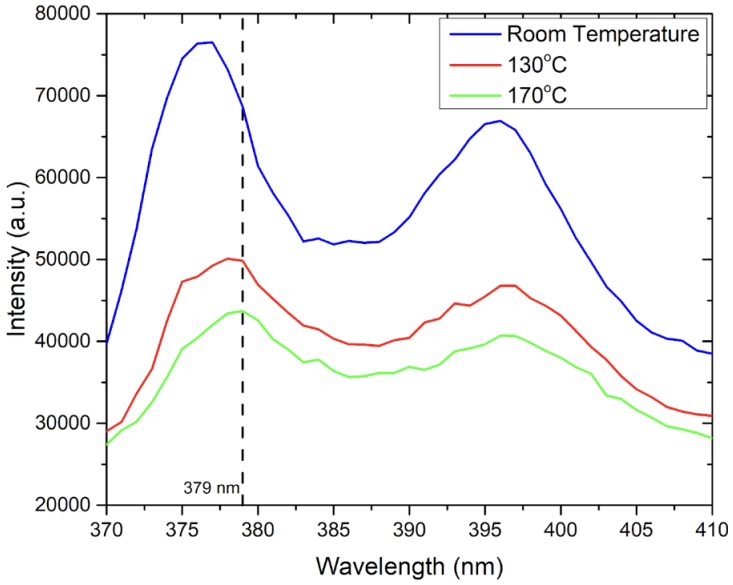

Figure 2.4: Representative emission spectra of pyrene dye taken at room temperature, 130^{o}C, and 170^{o}C. The spectra show the fluorescence emission intensity of the probe layer as a function of wavelength from 370 nm to 410 nm. The probe layer is covered by a bulk PS layer. The presence of grafted layer typically does not change the emission spectra of pyrene.

timescales much shorter than the fluorescence timescale. Therefore, the emitted photon when the electron returns to the ground state has a smaller energy than the photon absorbed by the electron during excitation, resulting in longer wavelengths of emitted photons compared to the excitation wavelength. This is known as the Stokes' Shift.[25]

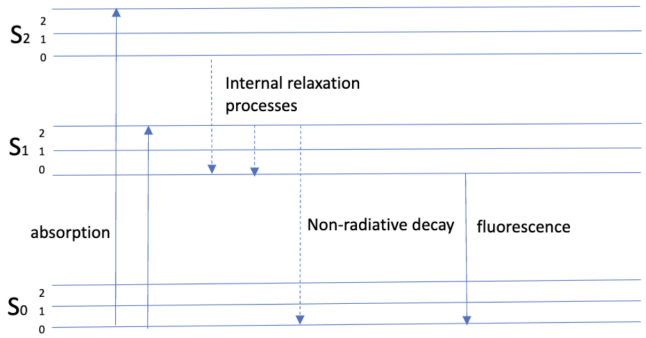

Figure 2.5: A simplified version of the Jabłonski diagram, which conceptually illustrates the excitation of electrons in a fluorophore to a higher energy state, the internal relaxation to the lowest vibrational and rotational state, followed by the return to ground state via fluorescence or non-radiative decay.

As shown in Figure 2.5, there are two main mechanisms for an electron to return to the

ground state from its excited state. One is emission of a photon via fluorescence, with a rate k_r. The other is non-radiative decay via processes such as vibrational relaxation, collision with surrounding molecules, formation of nonfluorescent complexes, with a rate k_{nr}. The quantum yield of fluorescence is defined as $Q = \frac{k_r}{k_r+k_{nr}}$. Ideally, the quantum yield is close to unity, where the fluorophore returns to the ground state solely via fluorescence, and hence the maximum fluorescence signal-to-noise ratio can be obtained in a measurement. The fluorescence lifetime is defined as $\tau = \frac{1}{k_r+k_{nr}}$. This is another important parameter of a fluorophore. As the fluorescence intensity decays exponentially as $I(t) = I_0 e^{-\frac{t}{\tau}}$, the window for observing fluorescence is between $\frac{\tau}{100}$ and 10τ.[24]

Fluorescence labeling as a way of sensing the glass transition of thin and ultrathin polymer films was established by Ellison and Torkelson.[14] At higher temperatures, due to the increased rate of thermal quenching, such as by collision with the surrounding molecules, vibrational relaxation from the excited state to the ground state via non-radiative decay increases, and therefore the quantum yield decreases, leading to a lower fluorescence emission intensity.[14] For pyrene in polymer matrices, the fluorescence emission intensity vs. temperature, $I(T)$, is a negative linear correlation. However, there is a break in the linear relationship at T_g associated with the change in mobility of the surrounding molecules that impact the rate of non-radiative relaxation above and below T_g.[6,14]

Such a break in the $I(T)$ relationship when the polymer changes from the liquid state to the glassy state makes pyrene fluorescence a useful probe for polystyrene thin film glass transition. T_g can be determined by linear fits of the $I(T)$ data for $T > T_g$ and $T < T_g$ separately, and then finding the intersection of the two lines.[14] As an illustration, Figure 2.6 is a T_g run of a pyrene-labeled PS layer next to bare silica substrate capped by 590 nm bulk PS. For multiple molecular weights of PS and PS pyrene label, the T_g found using fluorescence is consistent with the T_g measured by differential scanning calorimetry (DSC), establishing fluorescence as a reliable experimental technique for T_g measurements.[5]

2.3 Our Fluorescence Spectroscopy Method of Sensing the Glass Transition

In this project, fluorescence measurements were carried out using a Photon Technology International QuantaMaster spectrofluorometer. The assembled sample was held in a heater which was connected to an INSTEC temperature controller that reads real-time temperature of the sample and allows for temperature setting by the user. A clean optical quality quartz slide was placed atop the sample. To ensure that the sample is of sufficiently high quality, emission spectra were taken at room temperature after the sample had been placed into the spectrofluorometer, with an excitation wavelength of 332 nm, bandpass of 6 nm and slit width of 12.5 mm. If the emission spectra were noisy, the orientation of the sample would be adjusted until a spot had been found which would result in the least noise. Subsequently, the sample would be heated to 130^oC and annealed for 20 minutes. The purpose of this annealing is to remove air gaps and remaining water droplets after placing the bulk PS film, thus eliminating the free surface in the pyrene-labeled PS layer. In addition, heating the sample up to 130^oC would remove its thermal history, so the glass transition temperature measured should theoretically be consistent across all samples.[17] Subsequently, an emission scan spectrum would be taken at 130^oC using the same parameters as room temperature to observe the quality of the pyrene dye.

In order to measure T_g of the pyrene-labeled PS film, the sample was heated to and stabilized at 170^oC. An emission spectrum was taken immediately prior to collecting temperature-dependent fluorescence data. Figure 2.4 shows the emission spectra taken at room temperature, 130^oC and 170^oC before measurement. The spectrofluorometer detects the emission intensity at 379 nm, which corresponds to the peak emission intensity of pyrene at high temperatures. For the first couple of measurements, the temperature of the sample ramped steadily at 1^oC/min from 170^oC to 70^oC. In later measurements, in order to collect more fluorescence intensity data for fitting the T_g, the temperature range was changed to and fixed at from 170^oC to 50^oC. Because the T_g of bulk PS is well higher than 70^oC, this change will not alter the fitted T_g. Pyrene was excited at 332 nm with a bandpass of 4 nm and the emission intensity of pyrene at 379 nm was recorded

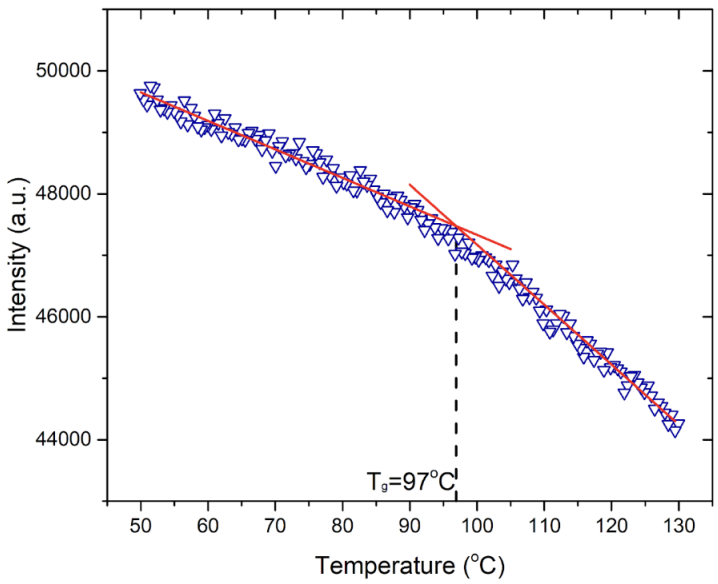

Figure 2.6: T_g Run from 130^oC to 50^oC to verify that fluorescence yields a reliable measure of T_g. Linear fit of this $I(T)$ graph of a 12 nm pyrene-labeled film on the quartz substrate without the grafted layer and capped by a 590 nm bulk PS layer obtained $T_g = 97^o$C, consistent with $T_{g,bulk}$ within an error of 3^oC.

every 3 in 30 seconds using a bandpass of 6 nm and slit width of 12.5 mm. Temperature dependence of corrected emission intensity of pyrene was analyzed in Origin. T_g was determined by linearly fitting to $I(T > T_g)$ and $I(T < T_g)$, and locating the temperature at their intersection. At the end of each T_g run, the sample was reheated to 170^oC and the post-run emission spectrum was taken and compared to one pre-run. This would check whether photobleaching of pyrene dye had occurred during the temperature ramp. Photobleaching would cause permanent decrease in the fluorescence capability of pyrene, and result in deviations from a linear dependence of $I(T)$ and thus uncertainties in T_g. For all the samples whose $I(T)$ graph was fitted to obtain the T_g, the pre-run and post-run emission spectra largely overlap, indicating that pyrene had not deteriorated during the run. If the post-run emission spectra showed more than 5% reduction in the emission intensity at 379 nm, extra cautions would be taken when fitting the data, and in most cases the data obtained from the sample would be discarded.

The T_g obtained with this method is shown to be consistent with the T_g obtained using an integrated intensity fluorescence method, similar to that used by Torkelson's group. Their method

involves integration of pyrene emission spectra from 350 to 450 nm using 1s/nm integration time. The integrated intensity was collected every 5K of cooling by taking emission spectrum of pyrene at every 5K intervals.[5,14] This method minimizes noise in the emission intensity measurement, but may introduce photobleaching to the pyrene dye, which is the permanent loss in fluorescence capability of the dye, especially at high temperatures. In conducting the control experiment to demonstrate the validity of our fluorescence method, we modified Torkelson's method by reducing the integration time to 0.3 s/nm, which keeps the total duration of pyrene exposure to excitation to be roughly equal with our method. Also, we observed that the pyrene emission spectra became noisy at around 360 nm and 450 nm, so we took the emission spectra from 370 to 430 nm instead.

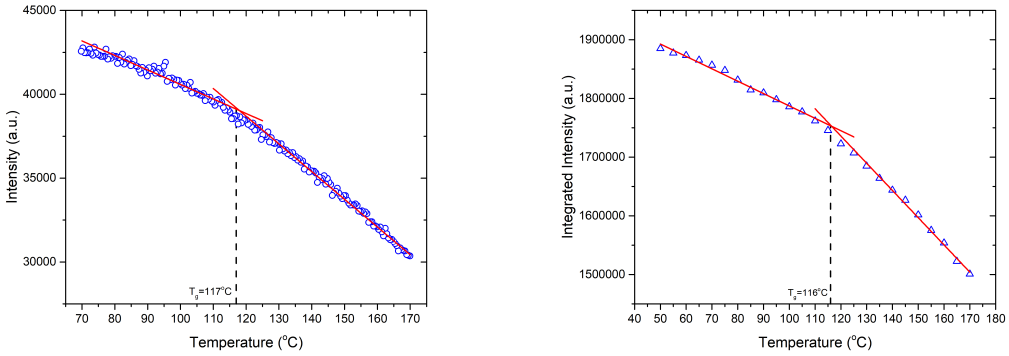

(a) (b)

Figure 2.7: Representative data that show the comparison of the T_g values obtained using our method of measuring the temperature-dependent pyrene emission intensity at 379 nm, which yielded $T_g \approx 116^o$C, as in (a), and the T_g fitted using the integrated intensity method similar to the one Torkelson and coworkers adopted, which yielded $T_g \approx 117^o$C, as in (b). The difference of 1^oC is negligible and likely due to noise in the measurement.

The merit of the integrated fluorescence intensity method is that, for a 170^oC to 50^oC temperature ramp, the integrated intensity vs. temperature graph obtained using this method contains only 25 data points, as opposed to 240 data points using our temperature ramping method. Hence the uncertainty in T_g fitted using the integrated fluorescence intensity method was smaller. Figures 2.7a and 2.7b show the fitted T_g of PS above 50 kg/mol grafted layers. The two methods yielded T_g values 117^oC and 116^oC respectively, and across multiple samples which I compared the T_g obtained using these two methods, the fitted T_g are within a difference of 1^oC. The consistency of

T_g values measured with our experimental method and a method adapted from the one in a well-established publication indicates that our experimental technique is a reliable way to measure T_g of PS thin films.

CHAPTER 3

RESULTS AND DISCUSSION

All the T_g run data was saved on the computer that operates the International QuantaMaster spectrofluorometer and the INSTEC temperature controller. After each measurement, the corrected emission intensity vs. time graph on the spectrofluorometer was exported and transferred into Origin for fitting. Since temperature ramps linearly at 1K/min, the intensity vs. temperature relation could be easily derived. In most graphs, the change of slope in I(T) at the transition of liquid to glassy state can be spotted by inspection, and the fitting window for each regime was chosen to reduce the residual sum of squares as much as possible.

3.1 Control Experiments

In order to confirm that any change in T_g was the result of grafting but not some alternative factors during the sample preparation steps, I performed control experiments by measuring the local T_g above the bare silica substrate without the grafted layer, equivalent to the sample geometry in the figure 3.1.

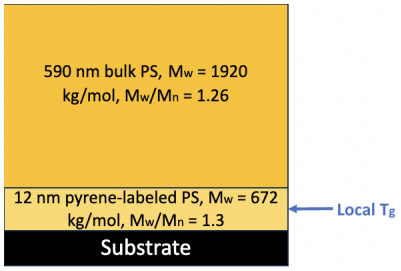

Figure 3.1: The assembly of the 12 nm pyrene-labeled PS above the silica substrate, capped by a 590 nm bulk PS. The T_g of the 12 nm PS layer should be approximately equal to $T_{g,bulk}$.

The alternative factors during the sample preparation procedure that could possibly lead to significant rise in T_g above $T_{g,bulk}$ are crosslinking of the probe layer and vacuum annealing of the probe layer at 170^oC for two hours. UV crosslinking causes bonding between different chains in the

matrix. Although high crosslinking density can restrict segmental mobility and cause increases in the T_g of the polymer,[26] our crosslinking procedure applies a much smaller amount of crosslinking just to prevent diffusion of the chains at high temperatures. Thus, our crosslinking of 10 minutes should not impact the glass transition.[11] The 2-hour annealing step at 170^oC was incorporated to allow interpenetration of the end-grafted chains into the PS matrix. Studies in the literature have claimed that annealing at high temperatures causes chain adsorption to the substrate, which is supposed to increase the amount of segments "sticking" to the surface. However, our group has not found that annealing a PS thin film to its substrate will change its T_g.[9]

To confirm that the elevation in the local T_g was not caused by crosslinking or 170^oC annealing, I prepared multiple samples without the grafted layer. Some probe layers were crosslinked for 10 minutes on mica prior to floating onto the silica substrate, and others were not. After transferring the probe layer onto silica, some samples were annealed for 2 hours under 170^oC vacuum. Overall, the control experiment resulted in four groups of samples: annealed and crosslinked, annealed but not crosslinked, not annealed but crosslinked, not annealed or crosslinked. In the control experiments, the temperature ramp was from 130^oC to 50^oC, rather than from 170^oC to 50^oC, because the purpose of these experiments is to verify the hypothesis that the measured T_g will be equal to $T_{g,bulk}$ approximately 100^oC. The plots in Figure 3.2 show the T_g run of the sample prepared via these protocols. These graphs show that neither crosslinking the pyrene-labeled PS film nor annealing at 170^oC of the PS film with the substrate changes the local T_g. Therefore, from these control experiments, we can conclude that the PS-COOH chains covalently bonded to the substrate is the cause of the increase in the local T_g of PS thin film, supporting the conclusion in the previous publications of our group.[11,17]

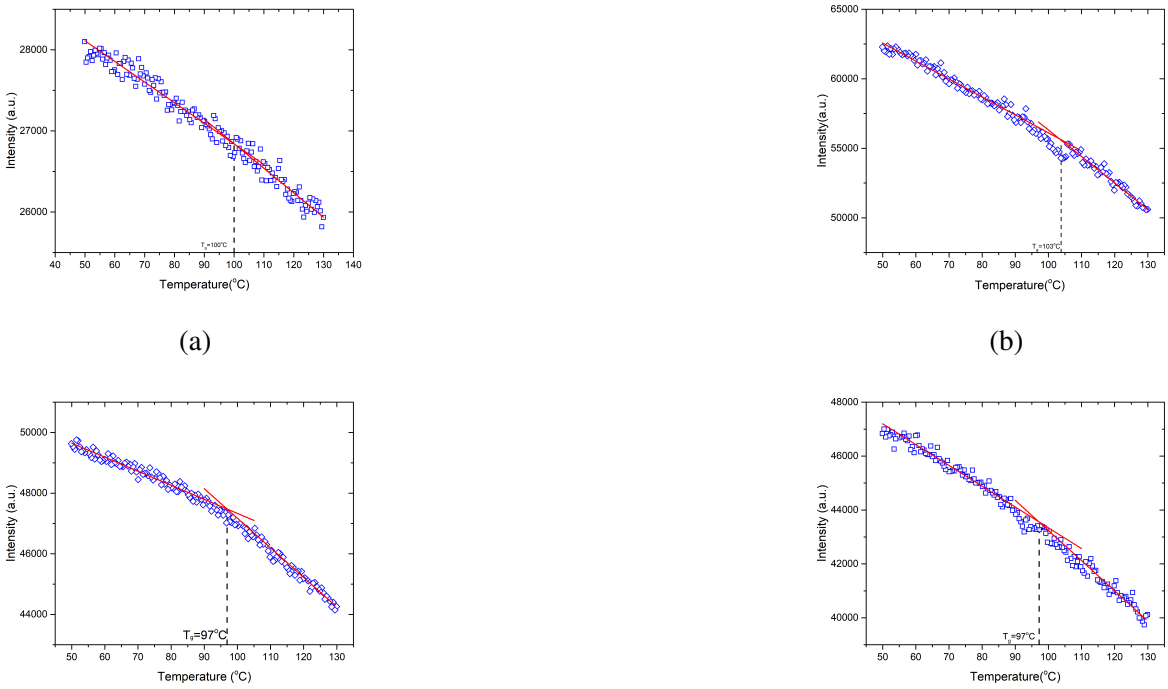

(a) (b)

(c) (d)

Figure 3.2: The four graphs are the T_g runs using the sample geometry shown in Figure 3.1, which is the control group without the grafted layer. Overall, the T_g recovers the value of $T_{g,bulk}$ to within 3^oC. Fitting of graph (a), which was the T_g of the sample prepared that involved the 10-minute crosslinking of 12 nm pyrene-labeled PS layer on mica, as well as the 2-hour annealing under 170^oC vacuum, resulted in $T_g = 100^o$C. Graph (b) corresponds to the sample prepared that was annealed for 2 hours, but not crosslinked, and the fitted T_g is 103^oC. Graph (c) corresponds to the sample prepared that was not annealed but crosslinked, which yielded $T_g = 97^o$C. Finally, Graph (d) corresponds to the sample prepared that was neither annealed nor crosslinked, which also yielded $T_g = 97^o$C.

3.2 Effect of End-Grafted Chains and Loops on the Local Glass Transition Temperature

3.2.1 Effect of Grafted Chains on the Local Glass Transition Temperature

I started by investigating the impact of end-grafted 100 kg/mol PS-COOH chain on the local T_g of PS matrices. The concentration of the toluene solution and spin speed of coating were modified to achieve different grafting densities. The probe layer and bulk PS cap layer were stacked onto the structure sequentially as described in Chapter 2. For all graphs in this section, the fitting window was chosen to be from 90^oC to 170^oC, and to truncate the data below 90^oC, in order to

match the analysis method adopted by Xinru Huang and James Merrill in publications.[11,17] Across multiple samples, the PS thin layer intermixed with 100 kg/mol end-grafted PS-COOH chains showed significantly elevated T_g from $T_{g,bulk}$. This suggests that the intermixing of matrix chains with end-grafted chains on silica substrates results in slower local dynamics in the polymer matrix. Figure 3.3 is a representative comparison of the T_g run of a pyrene-labeled PS layer above a bare silica substrate and above a substrate with 100 kg/mol end-grafted PS-COOH.

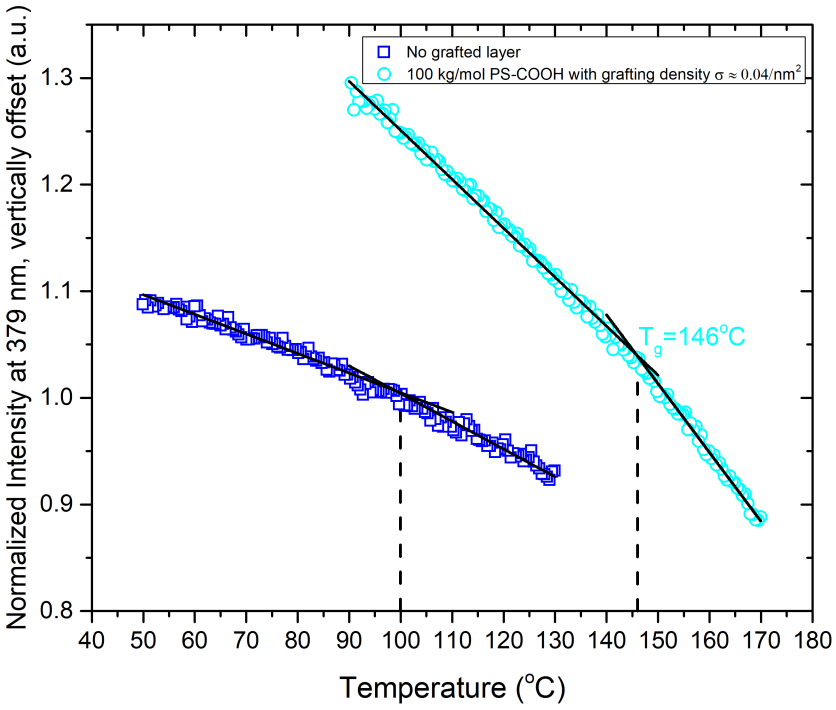

Figure 3.3: The T_g run of a sample without the grafted layer, from 130^oC to 50^oC, compared with the T_g run of a sample with 100 kg/mol end-grafted PS-COOH, at a grafting density of approximately 0.04 chains/nm^2, from 170^oC to 90^oC. While the T_g of the sample without the grafted layer is 100^oC, equivalent to $T_{g,bulk}$. With the grafted layer, the T_g increases dramatically to 146^oC.

In publications to date, the method to locate the T_g was primarily to visually inspect the approximate temperature at which the $I(T)$ relationship deviates from being linear. When I fit my obtained $I(T)$ graphs using the same method, I was successful in reproducing the same T_g values as the results published in ACS Macro Letters.[11] Huang and Roth suggested that there exists an ideal grafting density, $\sigma = 0.011$ chains/nm^2, that leads to the maximum increase in the local

T_g.[11] However, I collected more T_g data during summer 2021, with grafting density spanning from approximately 0.01 to 0.04 chains/nm^2. For 100 kg/mol PS-COOH chains, the radius of gyration R_g is 8.7 nm,[11] corresponding to $2.4 < \Sigma < 9.5$ based on the relationship $\Sigma = \pi R_g^2 \sigma$. My T_g measurements reveal that while the grafted layer causes an increase in the local T_g, the difference $T_g - T_{g,bulk}$ is roughly independent of the grafting density and fluctuates around 40^oC to 50^oC, as shown in Figure 3.4.

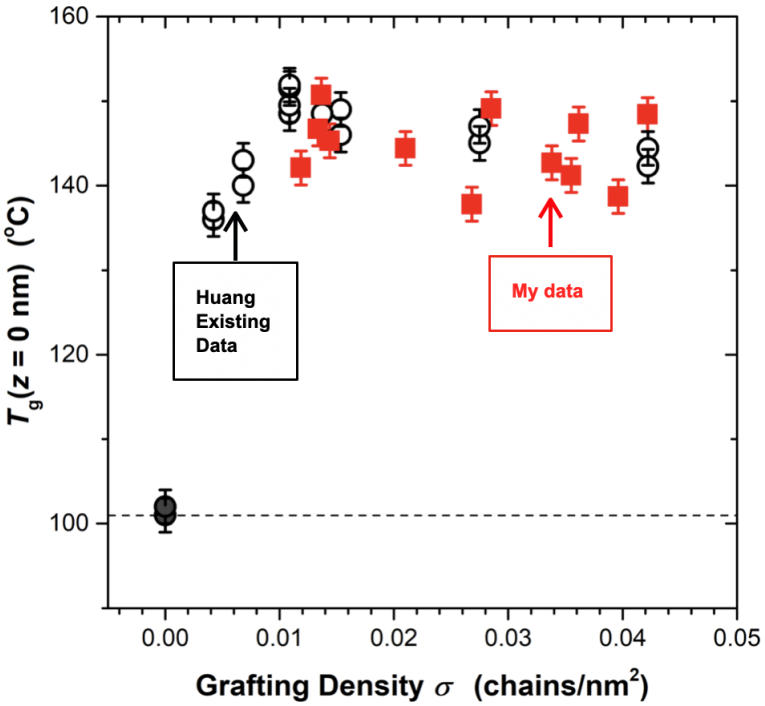

Figure 3.4: The T_g data I collected for 100 kg/mol end-grafted PS-COOH, as a function of grafting density. My data (in red solid squares) agree reasonably well with the data Huang and Roth published (in black hollow circles), showing significant increase from $T_{g,bulk}$ (in black solid circles).[11] The error bars in my measurement of T_g is set to be $\pm 2^o$C, consistent with the error bar used in the publication.

Although no significant relationship between grafting density and the local T_g was found, the molecular weight of the grafted chains may play a role. Smaller molecular weight of the grafted layer corresponds to shorter grafted chains, and hence shorter radius of gyration. Upon interpenetration into the matrix chains, the brushes are assumed to be in their ideal chain conformation, resulting in the penetration length $L \approx 2R_g \approx 17$ nm.[11] The R_g values are calculated as $R_g^2 = \frac{Nb^2}{6}$,

where b is the statistical segmental length and is equal to 0.67 nm for PS.[17] Therefore, grafted chains of 50 kg/mol have a penetration length of 6.2 nm into the matrix chains, and the shorter penetration length may impact the local T_g.

To compare the effect of 50 kg/mol and 100 kg/mol end-grafted PS-COOH chains, I replaced the 100 kg/mol PS-COOH grafted layers with 50 kg/mol end-grafted PS-COOH and measured the T_g of PS thin layers via fluorescence spectroscopy. Other than the difference in the molecular weight of the grafted layer, the samples were prepared with the same procedures. I adopted the same fitting method to obtain the T_g as I did for the 100 kg/mol grafted layer, so that the T_g values are comparable. From my measurement results that span across a range of grafting densities of 50 kg/mol PS-COOH, the local T_g does not differ significantly from when 100 kg/mol PS-COOH chains were grafted. The comparison of T_g for both molecular weights of the grafted chains is shown in Figure 3.5a. This discovery contributed to our December 2022 publication in ACS Macro Letter that I co-authored,[17] which found that the molecular weight of the grafted chains do not significantly influence the local T_g, as shown in Figure 3.5b. The figure includes some T_g data I collected for 50k and 100k PS-COOH, which I circled in black.[17]

From Figure 3.5b, there is no one single optimal grafting density that contributes to the maximum increase in the local T_g for both hydroxy (-OH) terminated and carboxy (-COOH) terminated PS chains of multiple molecular weights. Because of this finding, I assume that the grafting density is not an important parameter to alter in studying the glass transition, and hence when studying the grafted loop system, I shifted my focus to how intermixing time between the loops and the PS thin film may influence the local T_g.

3.2.2 Effect of Grafted Loops on the Local Glass Transition Temeperature

Our previous research suggests that, for single-end grafted chains, molecular weight and grafting density do not significantly impact the glass transition. Based on this discovery, for grafted loops, I did not characterize the grafting density dependence of the local T_g. However, Thees and coworkers proposed that smaller adsorbed loops may cause increases in the local T_g as they restrict

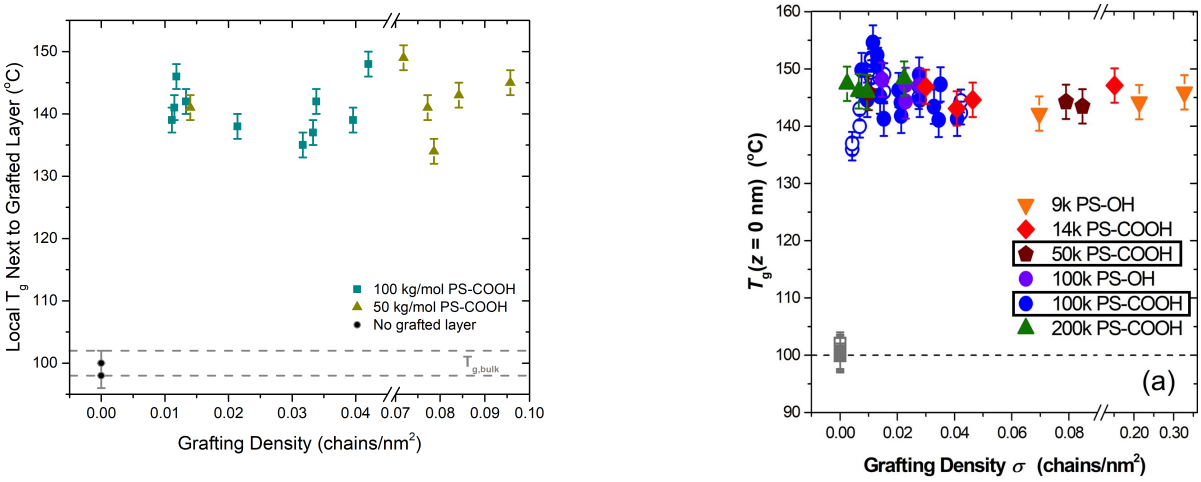

(a) (b)

Figure 3.5: (a) is my T_g measurements vs. grafting density for 50 kg/mol and 100 kg/mol PS-COOH end-grafted layers, and (b) is the image from the ACS Macro Letter article published in December 2022 by James Merrill, Ruoyu Li (me) and Connie B. Roth,[17] showing that the local T_g is independent of grafting density, and shows an abrupt increase from $T_{g,bulk}$ even when the grafting density is low. I collected the data for 50k (50 kg/mol) and 100k PS-COOH, as circled in black. James Merrill collected the T_g data for the rest of the grafted layers used. The results show that the local T_g is approximately 135^oC - 150^oC independent of the grafting density.

the mobility of the matrix chains, unlike fluffy loops. Therefore, I investigated the effect on the local T_g of 50 kg/mol and 100 kg/mol HOOC-PS-COOH loops. The difference in molecular weight corresponds to the difference in the size of the loops formed upon grafting. The method to fit the T_g with grafted loops was the same as the method to fit the grafted chains, namely, to fit over the range 90^oC to 170^oC, so that the T_g of PS intermixed with the grafted loops can be compared to the local T_g of PS intermixed with the adsorbed layers in the Thees et al. publication.[9] Figure 3.6 are the $I(T)$ graphs next to 50 kg/mol and 100 kg/mol grafted loops, of grafting densities 0.0660 chains/nm^2 and 0.0149 chains/nm^2 respectively. From the fits, T_g next to 50 kg/mol grafted loops is slightly higher than T_g next to 100 kg/mol grafted loops, both values are elevated compared to T_g next to the bare silica substrate. Compared to the local T_g next to end-grafted chains averaged over 10 samples, the average local T_g is lower by around 15^oC next to 100 kg/mol grafted loops, and around 6^oC next to 50 kg/mol grafted loops.

For loops covalently bonded to the substrate at both ends, I hypothesized that the local T_g

will depend on the intermixing time, as Thees and coworkers found in their article that sufficiently long annealing with the adsorbed chains adsorbed onto the substrate would lead to roughly 30K increase in the local T_g above $T_{g,bulk}$.[9] However, across multiple T_g measurements of the samples above the substrate with grafted loops, the local T_g does not appear to increase with the intermixing time between the 100 kg/mol grafted loops and the probe layer for 2 hours, 24 hours and 48 hours of annealing at 170^oC. Instead, the T_g data in Figure 3.7 show that, next to substrates with grafted loops, the local T_g increases by approximately $25-30^o$C compared to the substrate without grafted chains. Unlike melt-annealed adsorbed layers, the intermixing time does not significantly change the local T_g, indicating that the mechanisms by which grafted loops slow down the dynamics of the PS matrix chains are different from adsorbed loops.

In the Thees et al. work, tight adsorbed loops were found to increase the local T_g after long intermixing times, and the proposed mechanism of this increase is that the threading of the adsorbed loops by the PS chains over a long period of time at 170^oC causes slow down in the dynamics of the matrix chains.[9] The fact that the T_g does not depend on the intermixing time with grafted loops might be due to the size of the grafted loops. Thees and coworkers deduced that large fluffy adsorbed loops do not lead to increases in the local T_g even after long intermixing times.[9] One might reason that, similar to the adsorbed fluffy loops, if the grafted loops are too large, then increasing the intermixing time may not change the local T_g significantly. On the other hand, large adsorbed loops do not entail an increase in the local T_g, unlike grafted loops. This suggests that the chain connectivity to the substrate may play a defining role on the dynamics of the matrix chains, and that the 50 kg/mol and 100 kg/mol loops are 'fluffy', so the intermixing has limited effect on the T_g.

Figure 3.7 show my T_g measurements with grafted loops, compared with the samples on bare quartz substrate (control) that were annealed together with the substrate for up to 48 hours. Thees et al. publication found that the local T_g next to melt annealed adsorbed loops are 105 ± 2^oC for 2-hour intermixing, 128 ± 2^oC for 24-hour intermixing, and 131 ± 2^oC for 48-hour intermixing.[9] My measurements suggest that the local T_g next to grafted loops does not depend on the

intermixing time, and that smaller grafted loops may cause a higher T_g. A possible explanation of this difference is that smaller loops restricts the motion of matrix chains more than large loops, as Thees and coworkers reasoned for the tight adsorbed loops.[9] Nevertheless, more T_g measurements using different molecular weights of the grafted loops would be necessary to verify this conclusion.

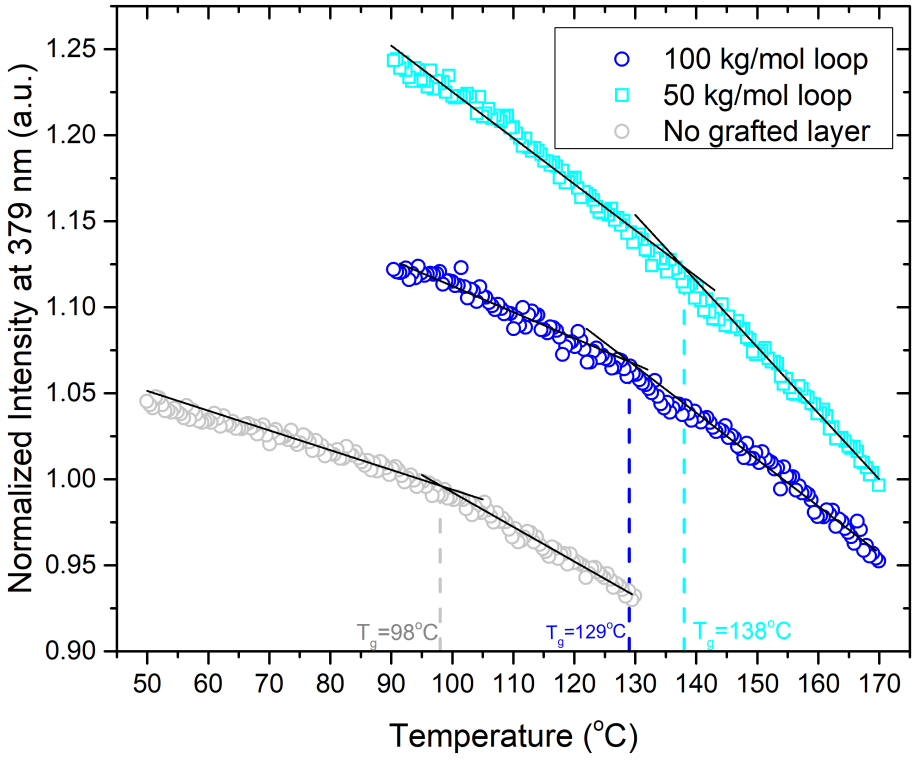

Figure 3.6: Comparison of the fluorescence intensity vs. temperature graphs of the pyrene-labeled PS layer next 50 kg/mol and 100 kg/mol grafted loops. The intermixing time was 2 hours, and the sample without grafted layer was annealed under 170^{o}C vacuum for 2 hours with bare silica substrate. $T_g = 138^o$C and 129^{o}C next to 50 and 100 kg/mol grafted loops, respectively. This is significantly elevated compared to T_g next to bare silica substrate, which is 98^{o}C, equal to $T_{g,bulk}$ within 2^{o}C.

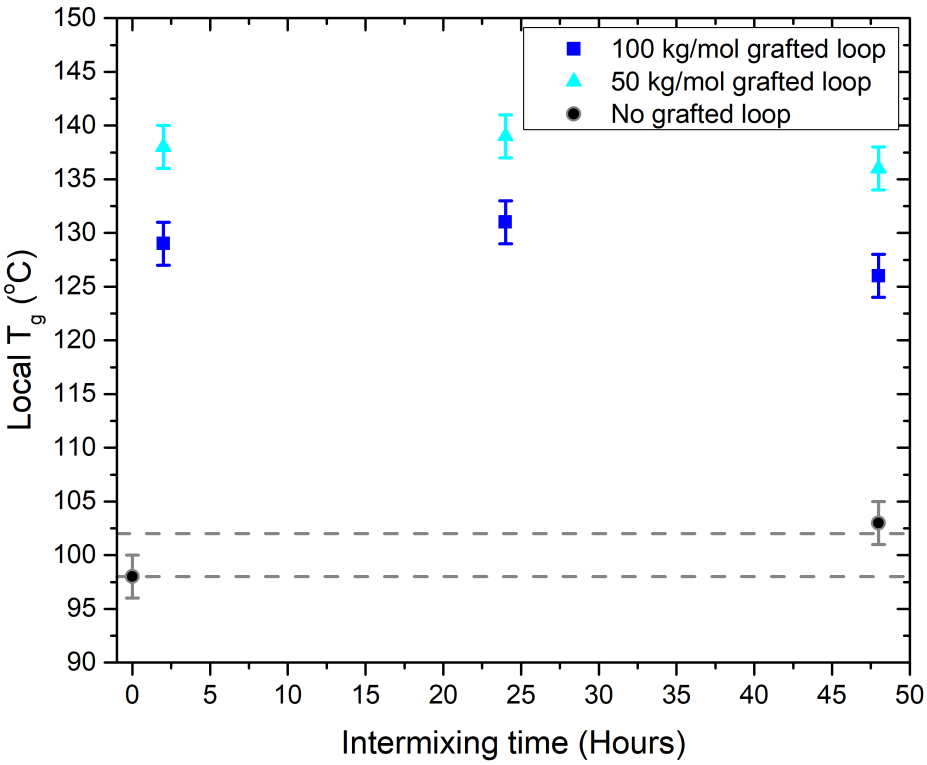

Figure 3.7: A plot of T_g vs. intermixing time for 50 kg/mol and 100 kg/mol grafted loop samples. The intermixing times are 2 hours, 24 hours and 48 hours. The samples are from the same batch as the ones that produce the graphs in Figure 3.6 The error bar is $\pm 2^o$C, consistent with those in the Thees et al. publication. From my findings, longer intermixing times do not entail higher T_g, and 50 kg/mol grafted loops cause greater increase the local T_g than 100 kg/mol grafted loops.

3.3 Discovery of Broad Glass Transition Over Extended Temperature Range

By identifying the T_g as the temperature at which the $I(T)$ relation starts to deviate from the linear relationship in the liquid state, we derived the T_g values in our publications so far. Namely, the starting point of the glass transition. In fact, the glass transition may in fact occur over a broad range of temperatures. When I and James Merrill revisited the $I(T)$ graphs, we noticed common occurrences of more than one change of the gradient of the intensity vs. temperature graph when we expand the fitting window to be from 50^oC to 170^oC. The fitting method we have been using to locate T_g had not captured this second transition. Nevertheless, the temperature at which the $I(T)$

relation first starts deviating from being linear can be a representative marker of the start of the glass transition, which may be understood as the 'onset' of glass transition. From our $I(T)$ graphs, each containing 199 or 239 data points for temperature ramps from 170^oC to 70^oC or 50^oC, if $I(T)$ graphs were to be fit over the entire temperature range, the temperature corresponding to the change in linearity will be different from when fitting from 90^oC to 170^oC. James Merrill developed an algorithm to fit for the T_g over the entire range of the temperature ramp, which allows for the choice of the fitting windows in the glassy and liquid states, and returns the T_g along with its uncertainty based on statistical calculations. For simplicity, the error of the T_g fit over the wide temperature range was kept at 2^oC. James Merrill is working on the more complicated task of identifying the error in this T_g and explain its significance. When I fit the $I(T)$ relation over the entire temperature range, I chose the fitting windows in such a way that minimizes the uncertainty in T_g, and omitting the segments of the graph that abnormally deviates from the normal trend, which might have been caused by large fluctuations in the intensity of the lamp of the spectrofluorometer. When the $I(T)$ graphs were fit in this manner, the T_g values were found to be lower, probably representing some midpoint temperature when the polymer transitions into the glassy state from the liquid state. We refer to the T_g fitted this way as T_g^{mid}. Figure 3.8 is a representative T_g run of a sample with 100 kg/mol grafted chains that can be fitted differently over the temperature range 50^oC to 170^oC and 90^oC to 170^oC. The T_g fitted over both ranges, and the resulting T_g values are both elevated compared to $T_{g,bulk}$.

Importantly, the broad glass transition only occurs in T_g runs next to grafted layers. There is no broad transition in the T_g runs of the PS layer next to bare silica substrate. The presence of two T_g values suggests that grafted layers result in a continuous glass transition of the PS layer intermixed with the grafted layer, where the difference between these two T_g values, $\Delta T_g = T_g - T_g^{mid}$, may provide some measure of the breadth of temperature over which the glass transition occurs. Since the $I(T)$ relationship of pyrene depends on the surrounding environment, the temperature corresponding to the first deviation of linearity in the liquid state, T_g, may be the temperature at which the surrounding environment of pyrene starts to densify and the glass transition starts. This

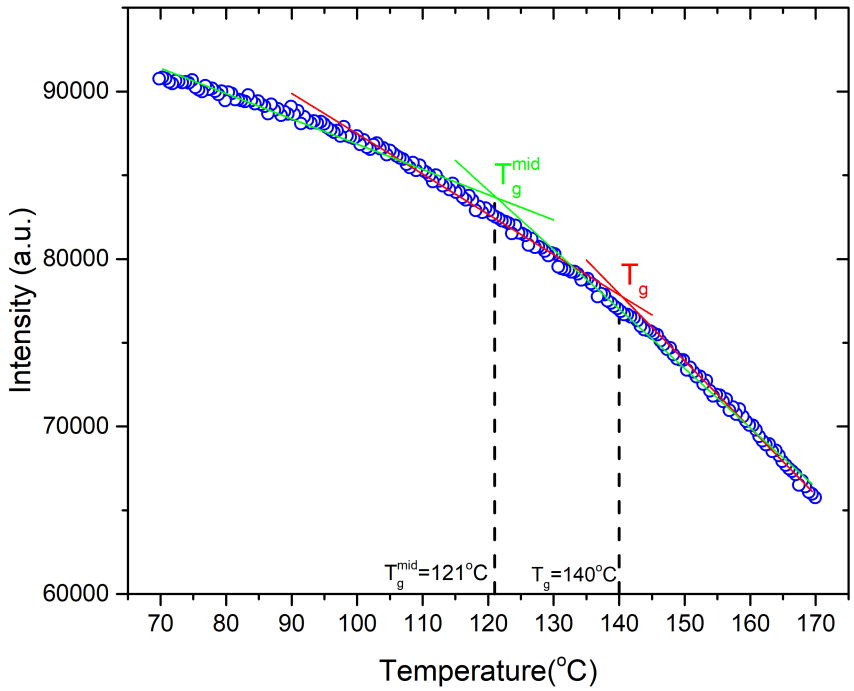

Figure 3.8: Fitting of an $I(T)$ graph of the T_g run of a sample with 100 kg/mol PS-COOH end-grafted layer. The graph is fitted in two ways. $T_g = 140^o$C (linear fits in red) was derived by fitting the graph from 90^oC to 170^oC, which was the temperature range chosen to fit the $I(T)$ relationship by Xinru Huang,[11] and the value of 140^oC is consistent with our published results. $T_g^{mid} = 121^o$C (linear fits in green) was obtained by fitting over the entire temperature range, from 70^oC to 170^oC.

transition continues over a range of temperature, although only one transition can be seen in the temperature range of above 90^oC. Over a broad temperature range in the cooling process, the $I(T)$ graph shows a flattening of the data. Our data show that the glass transition does not finish when temperature drops to below 90^oC. The temperature at which the glass transition terminates, the 'ending' of the glass transition, may be difficult to be precisely determined based on the $I(T)$ graph as the linear temperature dependence of intensity becomes noisier around the lower temperatures for many T_g measurements. All in all, the presence of T_g^{mid} is a recent discovery in addition to my results, and its physical significance is yet to be verified.

3.3.1 The "Midpoint" Glass Transition Temperature of Grafted Chains

The "midpoint" glass transition temperature of grafted chains, T_g^{mid}, is more spread out over multiple samples, but is still approximately independent of the grafting density and molecular weight, as plotted in Figure 3.9a. The difference ΔT_g also spans a large temperature range, although in general, ΔT_g values next to 50 kg/mol end-grafted PS-COOH chains are higher. This potentially means that glass transition next to 50 kg/mol grafted layers occur over a broader temperature range. The error bar of ΔT_g is calculated by $\delta(\Delta T_g) = \sqrt{(\delta T_g)^2 + (\delta T_g^{mid})^2} = \sqrt{2^2 + 2^2} \approx 2.8^o$C.

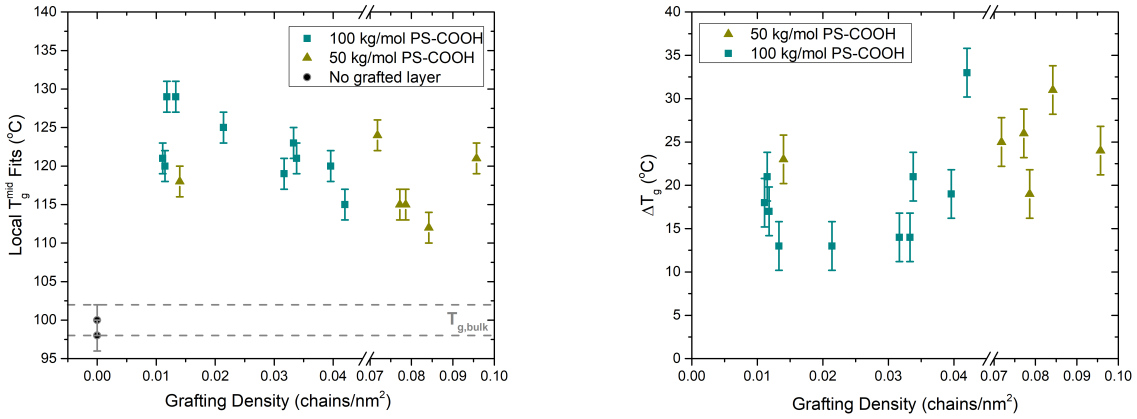

(a) (b)

Figure 3.9: Graph (a) shows the T_g^{mid} fits as a function of grafting density. The local T_g^{mid} values spread from approximately 110^oC to 130^oC. The error bar is assumed to be equal to the error bar to fit the T_g. (b) is the plot of ΔT_g as a function of grafting density, with an error bar of $\pm 2.8^o$C.

From the current data, ΔT_g does not significantly depend on the grafting density. However, more data is needed to draw a definitive conclusion about the relationship between the breadth of glass transition as a function of grafting density and the molecular weight of grafted chains.

3.3.2 The Midpoint Glass Transition Temperature of Grafted Loops

The T_g^{mid} values of PS intermixed with grafted loops were obtained by fitting over the entire range of the temperature ramp, so that the T_g^{mid} of the pyrene-labeled PS intermixed with

the grafted loops and chains can be adequately compared. Figure 3.10a compares the fit for the local T_g intermixed with the 100 kg/mol grafted HOOC-PS-COOH loops for 2 hours, 24 hours and 48 hours, each fit over the entire temperature range 50^oC to 170^oC, compared with the T_g next to bare silica substrate. The intermixing times of 2 hours, 24 hours and 48 hours result in the local $T_g^{mid} = 122^o$C, 119^oC and 118^oC, respectively, showing an elevation of approximately 20^oC above $T_{g,bulk}$. Figure 3.10b compares T_g^{mid} of PS intermixed with 50 kg/mol grafted loops. T_g^{mid} is 115^oC, 113^oC and 114^oC for intermixing times of 2 hours, 24 hours and 48 hours, respectively. Similar to T_g, T_g^{mid} does not depend on the intermixing time.

One interesting obervation is that while T_g, which corresponds to the onset of glass transition, is higher when PS is intermixed with 50 kg/mol grafted loops that when intermixed with 100 kg/mol grafted loops, T_g^{mid} is lower by roughly 5^oC when the PS is intermixed with 50 kg/mol than with 100 kg/mol grafted loops. On the other hand, T_g^{mid} values next to end-grafted chains are similar for 50 and 100 kg/mol end-grafted chains. More T_g measurements that employ different molecular weights of grafted loops are needed to elucidate the physical significance of this difference.

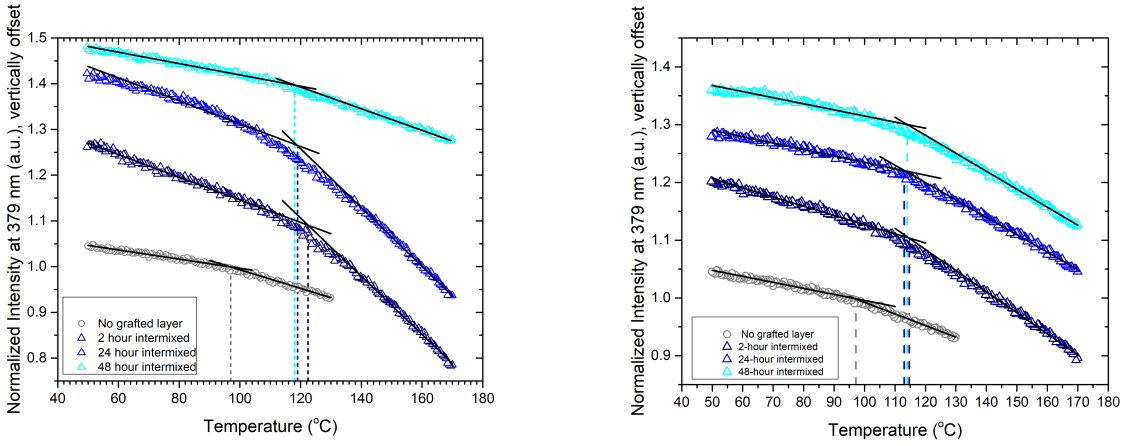

(a) (b)

Figure 3.10: Representative $I(T)$ plots of fluorescence intensity vs. temperature for 2 hours, 24 hours and 48 hours of intermixing of the pyrene-labeled PS layer and 100 kg/mol grafted loops, as in (a), or 50 kg/mol grafted loops, as in (b), compared to the sample without grafted layer. The intensity at the T_g of the sample without grafted layer was normalized to 1.0, while the other normalized data sets were vertically shifted for clarity.

Finally, I plotted T_g^{mid} vs. intermixing time for 100 kg/mol and 50 kg/mol grafted loops in Figure 3.11a, compared to T_g next to the bare silica substrate annealed for 0 and 48 hours, which is consistent with $T_{g,bulk}$. The plot shows that T_g^{mid} is lower for 50 kg/mol grafted loops than for 100 kg/mol grafted loop. The error bar used is $\pm 2^o$C. Figure 3.11b is the plot of ΔT_g vs. intermixing time, with an error bar of $\pm 2.8^o$C. ΔT_g for 50 kg/mol grafted loops is around 13^oC higher than for 100 kg/mol grafted loops, suggesting some mechanisms of 50 kg/mol grafted loops that cause glass transition over a much broader temperature range than 100 kg/mol grafted loops.

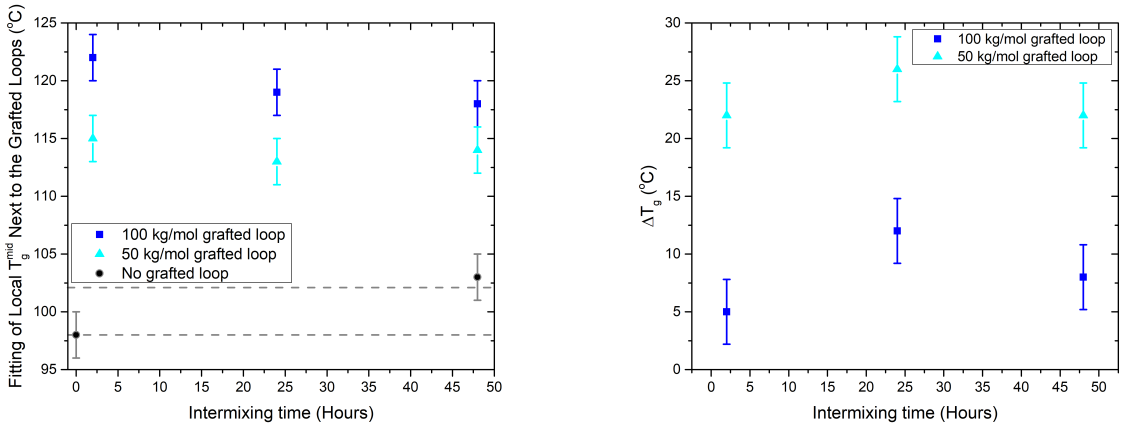

(a) (b)

Figure 3.11: (a): T_g^{mid} of PS vs. intermixing time with 100 kg/mol and 50 kg/mol grafted layers, and (b): plot of ΔT_g of PS vs. intermixing time with 100 kg/mol and 50 kg/mol grafted layers.

CHAPTER 4
CONCLUSION AND FURTHER WORKS

4.1 Summary of the Results

Over the course of more than two years, I researched extensively the impact of grafted layers on the local glass transition temperature (T_g) of 12 nm thick pyrene-labelled PS layers using fluorescence spectroscopy. Starting out with end-grafted PS-COOH chains, my results reliably suggest that end-grafted chains increase the local T_g compared to $T_{g,bulk}$. By changing the grafting density and the molecular weight of the grafted layer, I found that neither of the two factors influence the measured T_g significantly, which is in accordance with our published results.[17]

The motivation to study the T_g next to the grafted layer of dicarboxy-terminated PS loops arise from the Thees et al. publication,[9] which discovered that the local T_g increases with the intermixing time between the PS layer and the adsorbed layers formed by melt annealing, due to threading of PS matrix chains through the tight loops. I measured an increase in the local T_g next to the grafted loops, which is generally lower than T_g next to end-grafted chains, but still significantly elevated compared to $T_{g,bulk}$. Unlike adsorbed layers, the local T_g next to grafted loops does not change with the intermixing time. On average, the local T_g next to grafted loops is lower compared to next to grafted chains for both molar weights of 100 kg/mol and 50 kg/mol.

In addition to my main results, which agree with the published literature, by adopting a new fitting method, I found a lower T_g when I included a broader temperature range for fitting. To explain this difference, we propose that the T_g values in the publications are markers of the 'onset' of glass transition, while the lower T_g, which we denote T_g^{mid}, may represent the 'midpoint' of glass transition. T_g^{mid} values next to grafted loops and chains are not significantly different, but the difference $\Delta T_g = T_g - T_g^{mid}$ vary significantly from 5^oC to approximately 35^oC.

4.2 The Next Steps of the Project

In investigating T_g vs. grafting density for 100 kg/mol and 50 kg/mol grafted layers, I found no particular relationship between the two quantities. Therefore, future research regarding the effect of grafted layers on T_g may consider diverting the emphasis from grafting density. Compared to grafted chains, grafted loops are a relatively new system. From my findings, the local T_g next to 50 kg/mol grafted loops is higher than that next to 100 kg/mol grafted loops. There may exist a correlation between the molecular weight of the loops and the local T_g. Alternatively, the difference is simply some random fluctuation of T_g. It may be worth varying the size of the grafted loops to characterize how molecular weight of the loops impact the local T_g. In our December 2022 ACS Macro Lett. publication, James Merrill measured the local T_g next to 9 kg/mol, 14 kg/mol and 200 kg/mol in addition to 50 kg/mol and 100 kg/mol grafted chains.[17] T_g measurements could be done for grafted loops of these molecular weights as well.

Interestingly, while T_g is higher for 100 kg/mol than 50 kg/mol grafted loops, T_g^{mid} values is lower for 100 kg/mol than for 50 kg/mol grafted loops, and 50 kg/mol grafted loops seem to cause broader glass transition than 100 kg/mol grafted loops. This may reveal the impact of grafted layers on the glass transition over a broad temperature range. The difference $\Delta T_g = T_g - T_g^{mid}$ may provide some measure of the breadth of glass transition. Nevertheless, T_g^{mid} a new discovery. More T_g measurements and potentially new theory are needed to understand the physical significance of T_g^{mid} and what it reveals about the effect of grafted layers on the glass transition of PS.

REFERENCES

(1) Hiemenz, P. C.; P., L. T., *Polymer Chemistry*, 2nd ed.; CRC Press: Boca Raton, 2007; Chapter 1.

(2) Roth, C. B.; Baglay, R., *Polymer Glasses*; CRC Press: Boca Raton, 2016; Chapter 1.

(3) Roth, C. B., *Macromolecular Engineering: From Precise Synthesis to Macroscopic Materials and Applications*; Wiley: Online Library, 2022; Chapter Polymer Glasses.

(4) Giuntoli, A.; Puosi, F.; Leporini, D.; Starr, F. W.; Douglas, J. F. Predictive relation for the α-relaxation time of a coarse-grained polymer melt under steady shear. *Science Advances* **2020**, *6*, eaaz0777.

(5) Ellison, C. J.; Mundra, M. K.; Torkelson, J. M. Impacts of Polystyrene Molecular Weight and Modification to the Repeat Unit Structure on the Glass Transition Nanoconfinement Effect and the Cooperativity Length Scale. *Macromolecules* **2005**, *38*, 1767–1778.

(6) Ellison, C. J.; Torkelson, J. M. The distribution of glass-transition temperatures in nanoscopically confined glass formers. *Nature Materials* **2003**, *2*, 695–700.

(7) Jones, R. A. L.; Richards, R. W., *Polymers at Surfaces and Interfaces*; Cambridge University Press: Cambridge, England, 1999; Chapter 5-6.

(8) Milner, S. Polymer Brushes. *Science* **1991**, *251*, 905–914.

(9) Thees, M. F.; Merrill, J. H.; Huang, X.; Roth, C. B. Comparing the impact of different adsorbed layers on the local glass transition of polymer matrices. *The Journal of Chemical Physics* **2024**, *160*, 044908.

(10) Brittain, W. J.; Minko, S. A structural definition of polymer brushes. *J Polym Sci Part A: Polym Chem* **2007**, *45*, 3505–3512.

(11) Huang, X.; Roth, C. B. Optimizing the Grafting Density of Tethered Chains to Alter the Local Glass Transition Temperature of Polystyrene near Silica Substrates: The Advantage of Mushrooms over Brushes. *ACS Macro Letters* **2018**, *7*, 269–274.

(12) O'Connor, K.; McLeish, T. "Molecular velcro": dynamics of a constrained chain into an elastomer network. *Macromolecules* **1993**, *26*, 7322–7325.

(13) Aubouy, M.; Fredrickson, G.; Pincus, P; Raphaël, E End-Tethered Chains in Polymeric Matrices. *Macromolecules* **1995**, *28*, 2979–2981.

(14) Ellison, C. J.; Torkelson, J. M. Sensing the glass transition in thin and ultrathin polymer films via fluorescence probes and labels. *J Polym Sci Part B: Polym Phys* **2002**, *40*, 2745–2758.

(15) Hénot, M.; Chennevière, A.; Drockenmuller, E.; Shull, K.; Léger, L.; Frédéric, R. Influence of grafting on the glass transition temperature of PS thin films. *The European Physical Journal E* **2017**, *40*, 11.

(16) Thees, M. F.; McGuire, J. A.; Roth, C. B. Review and reproducibility of forming adsorbed layers from solvent washing of melt annealed films. *Soft Matter* **2020**, *16*, 5366–5387.

(17) Merill, J. H.; Li, R.; Roth, C. B. End-Tethered Chains Increase the Local Glass Transition Temperature of Matrix Chains by 45 K Next to Solid Substrates Independent of Chain Length. *ACS Macro Lett.* **2023**, *12*, 1–7.

(18) Bansal, A.; Yang, H.; Li, C.; Benicewicz, B. C.; Kumar, S. K.; Schadler, L. S. Controlling the Thermomechanical Properties of Polymer Nanocomposites by Tailoring the Polymer–Particle Interface. *J Polym Sci Part B: Polym Phys* **2006**, *44*, 2944–2950.

(19) Kumar, S. K.; Jouault, N.; Benicewicz, B.; Neely, T. Nanocomposites with Polymer Grafted Nanoparticles. *Macromolecules* **2013**, *46*, 3199–3214.

(20) Sukanek, P. C. Dependence of Film Thickness on Speed in Spin Coating. *J. of The Electrochem. Soc.* **1991**, *138*, 1712.

(21) Khodaparast, S.; Boulogne, F. m. c.; Poulard, C.; Stone, H. A. Erratum: Water-based Peeling of Thin Hydrophobic Films. *Physics Review Letters* **2018**, *121*, 269901.

(22) Tompkins, H. G.; Irene, E. A., *Handbook of Ellipsometry*; William Andrew: 2005; Chapter 1.

(23) Huang, X.; Roth, C. B. Changes in the temperature-dependent specific volume of supported polystyrene films with film thickness. *J. Chem. Phys.* **2016**, *144*, 234903.

(24) Valeur, B., *Molecular Fluorescence: Principles and Applications*; Wiley-VCH: 2001; Chapter 2-3.

(25) Lakowicz, J. R., *Principles of Fluorescence Spectroscopy*, 3rd ed.; Springer: 2006; Chapter 1.

(26) Zhang, Z.; Bai, P.; Xiao, Y.; Guo, Y.; Wang, Y. Conformation-Induced stiffening effect of crosslinked polymer thin films. *Communications Physics* **2023**, *6*, 332.